



OPEN ACCESS

EDITED BY

Jin Zhou,
Tsinghua University, China

REVIEWED BY

Zhangxi Hu,
Guangdong Ocean University, China
Barrie Dale,
University of Oslo, Norway

*CORRESPONDENCE

Juan B. Xillovich
✉ jbxillovich@ingeosur-conicet.gob.ar
Bernd Krock
✉ bernd.krock@awi.de

RECEIVED 11 December 2024

ACCEPTED 13 May 2025

PUBLISHED 04 June 2025

CITATION

Xillovich JB, Borel CM, Ferronato C and Krock B (2025) Distribution of organic-walled dinoflagellate cysts in surface sediments of San Matías Gulf (North Patagonian Shelf, Argentina): a seed bank for potential harmful algal blooms. *Front. Mar. Sci.* 12:1543414. doi: 10.3389/fmars.2025.1543414

COPYRIGHT

© 2025 Xillovich, Borel, Ferronato and Krock. This is an open-access article distributed under the terms of the [Creative Commons Attribution License \(CC BY\)](https://creativecommons.org/licenses/by/4.0/). The use, distribution or reproduction in other forums is permitted, provided the original author(s) and the copyright owner(s) are credited and that the original publication in this journal is cited, in accordance with accepted academic practice. No use, distribution or reproduction is permitted which does not comply with these terms.

Distribution of organic-walled dinoflagellate cysts in surface sediments of San Matías Gulf (North Patagonian Shelf, Argentina): a seed bank for potential harmful algal blooms

Juan B. Xillovich^{1*}, C. Marcela Borel¹, Carola Ferronato² and Bernd Krock^{3*}

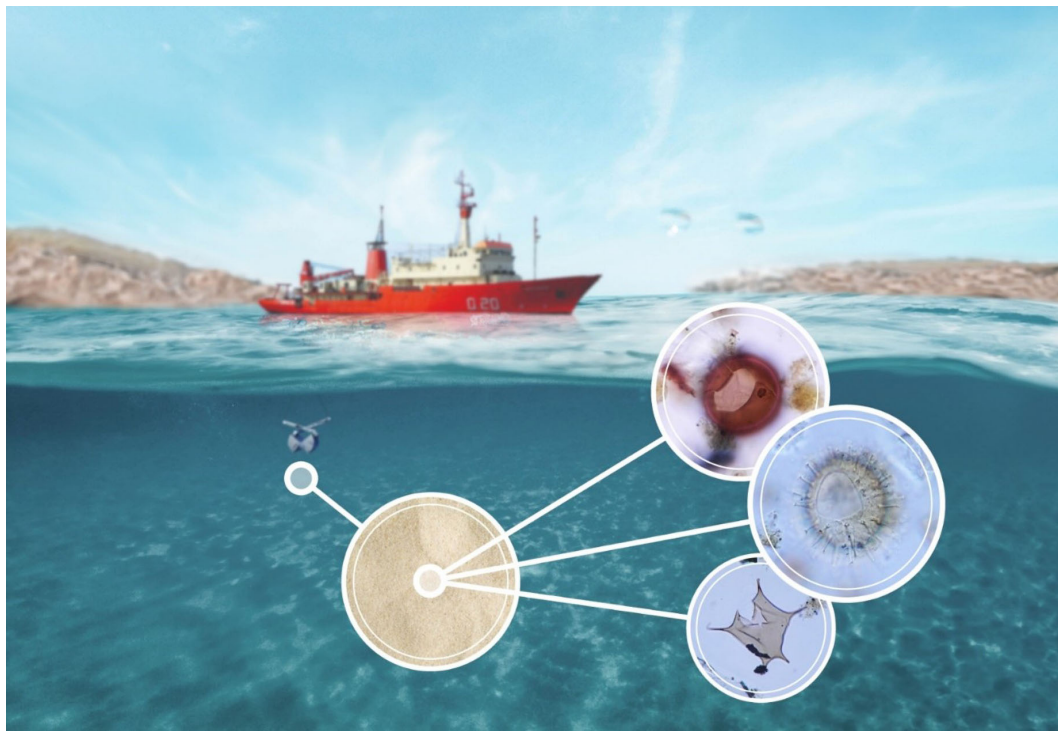
¹Instituto Geológico del Sur (INGEOSUR), Universidad Nacional del Sur-Consejo Nacional de Investigaciones Científicas y Técnicas (CONICET), Departamento de Geología, Bahía Blanca, Argentina,

²Instituto Argentino de Oceanografía (IADO), Universidad Nacional del Sur-Consejo Nacional de Investigaciones Científicas y Técnicas (CONICET), Bahía Blanca, Argentina, ³Ecological Chemistry, Alfred Wegener Institut-Helmholtz Zentrum für Polar- und Meeresforschung, Bremerhaven, Germany

In the southwestern Atlantic Ocean, the San Matías Gulf (SMG) is a semi-enclosed coastal ecosystem (40.5°–42.5°S; 63.5°–65.5°W) with considerably greater depths (up to 190 m) than the adjacent continental shelf (~70 m). A thermohaline frontal system develops in a latitudinal position around 41.8°S from spring to summer leading to high biological productivity in this relevant area for fisheries. In this study, twelve surface sediment samples from the SMG were analyzed for the determination of species and distribution of organic-walled dinoflagellate cysts (dinocysts) in relation to physico-chemical conditions (grain-size of sediments, water column stability, spring sea-surface temperature, salinity, and nitrate concentration). Thirty different taxa of dinocysts were recorded, of which twenty-eight were identified to species level. The strong dominance of *Operculodinium centrocarpum* (cyst of *Protoceratium reticulatum*, a yessotoxin producer in the Argentine Sea) accompanied by minor abundances of other phototrophic and heterotrophic taxa characterized all assemblages. Cysts of *Alexandrium catenella*, which is known as a saxitoxin-producing species in the gulf, were also recorded across sites. The highest absolute abundances of dinocysts occurred at the inner gulf, north of the latitudinal front. For this area we argue that multi-year fluxes of phototrophic dinocysts to the silty bottom are enhanced by the great production of vegetative cells in the seasonally stratified water column, the encystment strategies of the dominant species and the particular physical oceanographic characteristics. Although densities of both phototrophic and heterotrophic cysts were lower in the coarser sediments near the mouth of the gulf, the relative abundances of heterotrophic cysts were higher. The preference of heterotrophic species reflects higher nitrate concentrations, which increase the primary production and thus food availability for heterotrophs.

KEYWORDS

dinoflagellate cysts, environmental parameters, harmful algal blooms, Patagonian gulf, SW Atlantic



GRAPHICAL ABSTRACT

1 Introduction

Dinoflagellates are microscopic unicellular organisms occupying most aquatic environments, from freshwater bodies to open ocean and they constitute important primary producers, playing a central role in the planktonic food web (de Vernal and Marret, 2007). They can have phototrophic, heterotrophic or mixotrophic life strategies (Zonneveld and Pospelova, 2015). The phototrophic dinoflagellates depend upon light and dissolved nutrients (nitrogen and phosphorous, notably), and live in the photic zone at relatively shallow depths; while the heterotrophic ones depend upon the overall productivity and generally inhabit in surface waters where their preys occur (de Vernal et al., 2007). Mixotrophic species combine both strategies, being able to photosynthesize and also to switch into heterotrophic mode when environmental conditions are not favorable for photosynthesis (Hansen, 2011; Gilbert and Mitra, 2022).

During reproduction, as part of their life cycle, a number of marine and freshwater dinoflagellate taxa produce resting cysts that have the potential to become fossilized in sediments (Zonneveld and Pospelova, 2015). About 200 dinoflagellates have been shown to produce organic-walled resting cysts (dinocysts) and more than 20 of these cyst-producing dinoflagellates are known to cause harmful algal blooms (HABs) (Tang and Gobler, 2012). The dinocysts eventually sink to the seafloor and since they have a similar composition to the highly resistant sporopollenin in pollen grains, when preserved, they provide a fragmentary picture of original populations (de Vernal, 2009). Resting cysts involve a usually

obligatory period of dormancy which varies among species ranging from days to months (e.g., Kremp and Anderson, 2000; Figueroa et al., 2006). Dinocysts allow the survival of populations under environmental adverse conditions because their germination provides new vegetative cells to the water column. Many toxic and HAB species are cyst-forming especially those causing recurrent blooms (e.g. Ellegaard and Ribeiro, 2018). Therefore, dinocysts in sediments are considered as a “seed bank” since they constitute a storage for the occurrence of HABs (Anderson et al., 2012). Areas with the highest concentrations of dinocysts of potentially toxic species in the sediments are considered zones of risk for the initiation of new planktonic populations and future blooms of these microalgae (Brosnahan et al., 2017; Smayda, 2002).

The distribution and abundance of dinocysts principally depend upon upper water parameters such as sea-surface temperature, sea-surface salinity, nutrient availability, sea ice cover, prey distribution, deep dissolved oxygen, sediment redox and pH (Marret et al., 2019; Zonneveld et al., 2013 and references therein). In particular, since heterotrophic dinoflagellates feed on primary producers and notably on diatoms, the abundance of their cysts indirectly provides a signal of the primary productivity (de Vernal, 2009). Due to their sensitivity to such environmental factors, fossil dinocyst assemblages constitute useful proxies to reconstruct surface water conditions at times of the sediment deposition.

San Matías Gulf (SMG) is an important area for feeding, reproduction and resting of numerous migratory species of marine mammals and birds. Several economically important fish and cephalopod species develop their entire life-cycle within this

area, establishing populations which are autonomous from those in the contiguous Argentine sea (Crespi-Abril et al., 2008; Ocampo-Reinaldo et al., 2013; Romero et al., 2013; Svendsen et al., 2015). Therefore, the SMG is a critical feeding area where toxin-producing dinoflagellates impact pelagic food webs (Hoffmeyer et al., 2020; Sastre et al., 2018). In the region there have been records of HABs of *Alexandrium catenella* since 1980, mainly during spring causing closures of the collection of mollusks and leading in some cases to bird and marine mammal mortalities, and also to human deaths (Carreto et al., 1981; Esteves et al., 1992; Gayoso et al., 2006; named as *Gonyaulax excavata* or *A. tamarensis*).

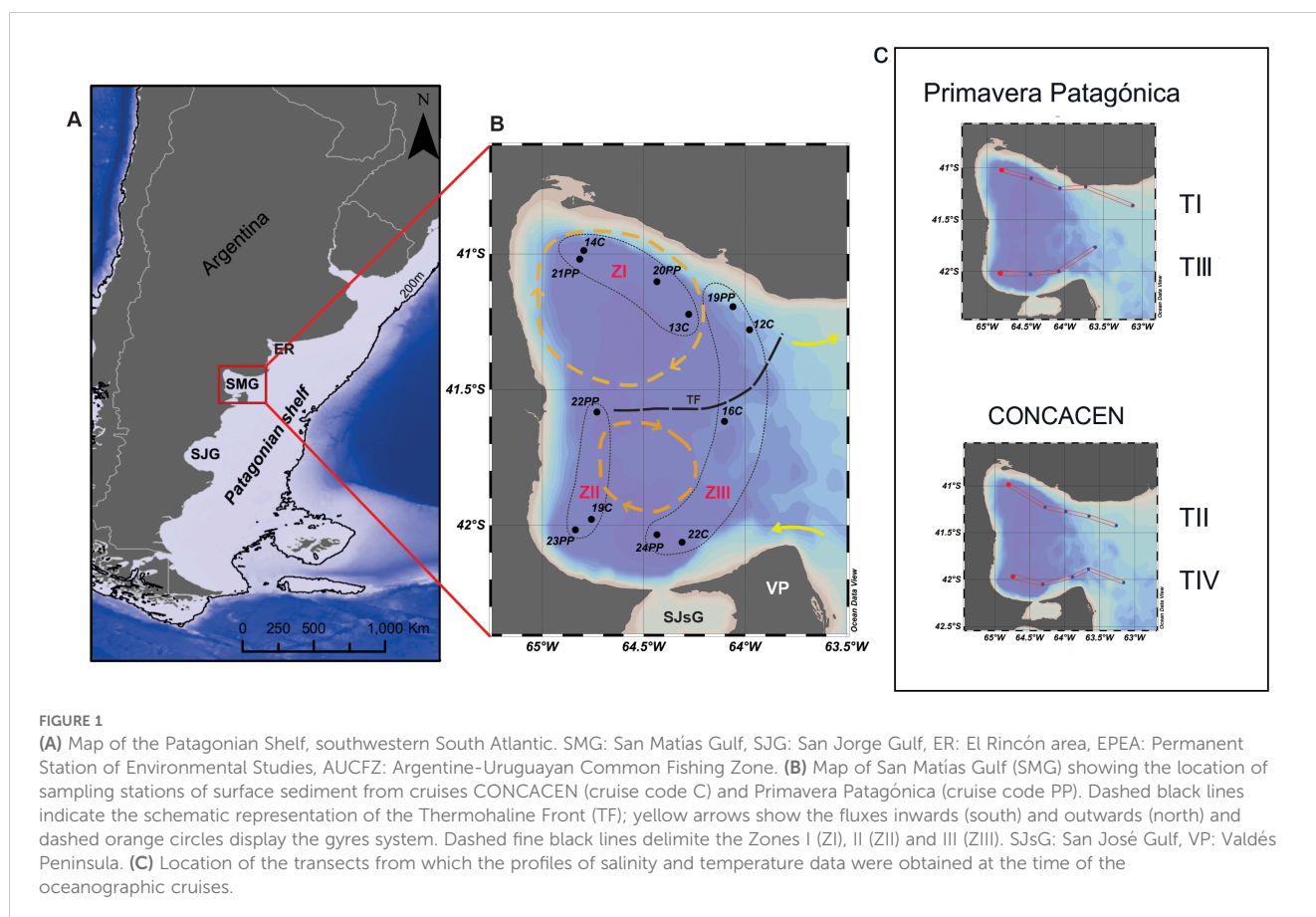
The aims of the present work are to describe the first record of dinocyst assemblages present in recent bottom sediments of SMG through their taxonomic study, and document the presence of the benthic phase of potentially harmful dinoflagellates. We hypothesize that the high abundances of dinoflagellate cysts in the bottom sediments of this gulf are influenced by its semi-enclosed nature and oceanographic characteristics, including a bathymetric threshold at its mouth, cyclonic gyres in the northern sector, and the cyst-producing potential of the most dominant species in the assemblages. For this purpose, we analyze the main environmental factors that drive the distribution and abundances of dinocysts herein and explore whether these factors influencing cyst assemblages are consistent across the entire gulf area. This work

also lays the groundwork for future paleoenvironmental studies using dinocyst records from Holocene sediment cores collected in the gulf.

2 Regional setting

The Southwestern Atlantic Shelf south of 40°S, known as the Patagonian Shelf of Argentina, features an extensive coastline with variable geomorphology, including bays, gulfs, and peninsulas. These characteristics contribute to the development of diverse marine frontal systems, which enhance primary and secondary productivity (Acha et al., 2015; Williams et al., 2021 and references therein), supporting rich and diverse planktonic dinoflagellate communities (e.g., Akselman, 1985, 1986; Balech, 1988; Antacli et al., 2018; Fabro and Almandoz, 2021). However, studies on dinoflagellate cysts (dinocysts) recovered from surface sediments of the Patagonian Shelf and their relationship with environmental parameters remain scarce (Akselman, 1987; Orozco and Carreto, 1989; Candel et al., 2012; Krock et al., 2015; Faye et al., 2018).

This study focuses on the San Matías Gulf (SMG), located on the northern Patagonian coast (Figure 1A), an area with high-priority conservation status. The gulf covers approximately 20,000



km² and communicates with the open sea through a 100 km long and ~70 m deep mouth (Mouzo and Paterlini, 2017). Its semi-enclosed nature and oceanographic characteristics, such as a bathymetric threshold at its mouth and cyclonic gyres in the northern sector (Figure 1B), significantly influence water circulation (Piola and Rivas, 1997).

The climate is semi-arid with scarce precipitation due to the forced subsidence of low level westerly winds over the eastern slopes of the Andes towards the temperate Argentinian Patagonian steppes, where the gulf is settled (Garreaud, 2009; Garreaud et al., 2009). The study area has an annual precipitation uniformly distributed (a relatively minor maximum in autumn and other in spring months) of ~250 mm, a mean annual temperature of about 13.5°C and a high potential evapotranspiration (Labraga and Villalba, 2009). The continental supply of fresh water is scarce and intermittent. There are two streams that flow into the gulf, the Green and the Salado, with negligible discharges. On its coasts the main urban centers (San Antonio Oeste, San Antonio Este, Las Grutas and Sierra Grande) with less than 30,000 inhabitants (INDEC, 2010) are within the department of San Antonio.

A W-E orientated front is established from late spring to summer around 41.8°S, separating the coldest waters in the south from the warmest waters in the northern sector (Saraceno et al., 2020). The oriental tip of the latitudinal thermohaline front extends towards the north along the gulf mouth forming a complex tidal frontal system linked to the characteristics of the bottom topography (Williams et al., 2021). Both tide and wind are also important for the formation of this zonal front (Tonini et al., 2013). The NW-N zone presents a cyclonic circulation with higher temperature and salinity and a strong stratification from spring to summer. The S-SE portion, influenced by the input of colder nutrient-rich and less saline shelf waters is subject to weak

stratification (Piola and Scasso, 1988; Gagliardini and Rivas, 2004; Tonini et al., 2013; Pisoni et al., 2015).

The surface distribution of nitrate in spring (October 2009) showed a heterogeneous pattern with low values in the SW of the gulf (max. 1 μM), medium in the NW-N zone (~1.9 μM) and maxima over the mouth (~ 4 μM in the south of the mouth) following the input of colder, fresher and nutrient rich waters from the adjacent shelf (Williams et al., 2021). During summer, nitrate values were lower (max. 0.5 μM) and homogeneous all over the gulf (Williams et al., 2021). Locally, high nitrate levels were measured in San Antonio Bay, due to human settlement in that small area of the northern SMG (Martinetto et al., 2010).

For spring months (September-November), the satellite images of chlorophyll-a (Chl-a-sat) also showed a heterogeneous pattern with higher values (3.5 to 8.0 mg m⁻³) in the inner SW-S sector of the gulf and in the south of its mouth. High concentrations were also observed in the inner NW-N sector but with a patchy pattern. During summer the Chl-a-sat decreases throughout the gulf, with minimum values in the NW-N enclosed sector where the thermocline establishes. The NW-N region displays another Chl-a-sat maximum in autumn (April-May) coincident with the end of the water column stratification (Williams et al., 2021).

3 Materials and methods

3.1 Oceanographic cruises, sample collection and *in situ* measurements

Twelve bottom sediment samples were collected during two oceanographic cruises on board of the R/V Puerto Deseado (CONICET-MINDEF, Argentina): six samples during

TABLE 1 Cruise, geographical coordinates and depths of the surface sediment samples and corresponding sediment types (according to Shepard, 1954).

Station	Cruise	Latitude (S)	Longitude (W)	Depth (m)	Sediment grain size (%)			Sediment type
					Clay	Silt	Sand	
14C	CONCACEN R/V PD 2009	-40.988	-64.796	129	12	62	26	Sandy silt
21PP	Prim. Pat. R/V PD 2013	-41.020	-64.818	131	8	54	38	Sandy silt
20PP	Prim. Pat. R/V PD 2013	-41.100	-64.434	133	11	54	35	Sandy silt
13C	CONCACEN R/V PD 2009	-41.226	-64.279	125	8	52	40	Sandy silt
22PP	Prim. Pat. R/V PD 2013	-41.580	-64.731	162	21	65	14	Clayey silt
19C	CONCACEN R/V PD 2009	-41.977	-64.763	149	0	98	2	Silt
23PP	Prim. Pat. R/V PD 2013	-42.019	-64.868	127	15	47	38	Sandy silt
19PP	Prim. Pat. R/V PD 2013	-41.194	-64.065	86	4	16	80	Sand
12C	CONCACEN R/V PD 2009	-41.274	-63.976	83	9	33	58	Silty sand
16C	CONCACEN R/V PD 2009	-41.612	-64.105	103	10	28	62	Silty sand
24PP	Prim. Pat. R/V PD 2013	-42.030	-64.434	182	8	21	71	Silty sand
22C	CONCACEN R/V PD 2009	-42.062	-64.313	157	12	31	57	Silty sand

CONCACEN (cruise code C) in November 2009 and six samples during Primavera Patagónica (cruise code PP) in November 2013 (Figure 1B). Sediment samples for palynological analyses (Table 1) were taken from the top centimeter of the sediment collected in a 0.003 m³ Wildco® Shipek grab (between 83 and 182 m depth) and kept in dark and cool (4°C) conditions to prevent cyst germination. In addition to sediment sampling, continuous profiles of temperature and salinity were recorded using a Sea-Bird SBE-19 plus V2 CTD of the Servicio Hidrografía Naval (SHN, Argentina) and calibrated with a final precision of 0.05 in salinity and 0.02°C in temperature.

3.2 Palynological analyses

An aliquot of wet sediment samples (between 11.5 and 35 g for each station) were sieved through 150 and 10 µm Nitex® screens to eliminate clay and fine silt (<10 µm), and coarse grained (>150 µm) particles. Two calibrated tablets of *Lycopodium clavatum* (University of Lund, BATCH N° 483216) containing 18,583 spores were added to each sample as an internal standard (Stockmarr, 1971) to allow the calculation of absolute abundances of dinocysts (cysts g⁻¹ wet sediment) from the counts of the marker spores and cysts. The 10-150 µm grain size fraction was treated sequentially under room temperature with 10% hydrochloric acid (HCl) and 49% hydrofluoric acid (HF) to dissolve carbonate and silicate phases, respectively. For preservation of dinocysts neither alkaline solutions nor acetolysis were used. The organic residues

were mounted on glass slides in Kaiser gelatine-glycerine and covered with cover slips for optical microscopic analysis (Marret and Zonneveld, 2003; de Vernal et al., 2010). Slides (LPUNS) are stored at the Colección Palinológica, Laboratorio de Palinología (INGEOSUR-UNS), Bahía Blanca, Argentina.

Dinocysts were identified and systematically counted using a Nikon 80i transmitted-light microscopy at 400–1000 x magnification. Dinocyst images were taken with a Nikon Coolpix 950 digital camera. The nomenclature of the dinocysts follows Fensome et al. (1993). The paleontological taxonomy of dinocysts differs from the biological taxonomy of motile stages due to a history of separate research. The paleontological names are used throughout this text and the biological affinities for the species counted are given in Tables 2, 3. Specimens were classified to the genus level where species-level identification was not possible. The specimens of *Operculodinium centrocarpum* sensu Wall, 1967 with “normal” processes (10-11 µm long) were separately counted from those of “intermediate” processes (2 to 7 µm long) and “short” truncate processes (< 2 µm long). Specimens of *Spiniferites* that could not be identified to species level were grouped as *Spiniferites* spp. *Polykrikos kofoidii* and *Polykrikos schwartzii* cysts were counted together as *Polykrikos kofoidii/schwartzii* complex because of intergradation between the ornamentation that characterizes both species, which makes it difficult to distinguish between the taxa unambiguously. In the category *Brigantedinium* spp. were grouped round to ovoid brown cysts resembling *B. cariacense* and *B. simplex* but which could not be identified at the species level because their polygonal archeopyle was obscured or only partially seen.

TABLE 2 List of phototrophic (including mixotrophic) dinocyst taxa (theca- and cyst-based names) identified for SMG in this study.

Family/Subfamily	Cyst-based name (paleontological)	Theca-based name (biological)	
Gonyaulacaceae	Cribroperidinioidae	<i>Operculodinium centrocarpum</i> (Deflandre et Cookson) sensu Wall, 1967	<i>Protoceratium reticulatum</i> (Claparède et Lachmann) Bütschli, 1885
		<i>Operculodinium israelianum</i> (Rossignol) Wall, 1967	<i>Protoceratium reticulatum</i> (Claparède et Lachmann) Bütschli, 1885
	Gonyaulacoideae	<i>Achomospaera</i> sp.	? <i>Gonyaulax</i> sp.
		<i>Spiniferites belerius</i> Reid, 1974	<i>Gonyaulax scrippsae</i> Kofoid, 1911
		<i>Spiniferites bulloideus</i> (Deflandre et Cookson) Sarjeant, 1970	<i>Gonyaulax scrippsae</i> Kofoid, 1911
		<i>Spiniferites lazus</i> Reid, 1974	<i>Gonyaulax</i> sp.
		<i>Spiniferites ludhamensis</i> Head, 1996	unknown
		<i>Spiniferites mirabilis</i> (Rossignol) Sarjeant, 1970	<i>Gonyaulax spinifera</i> complex
		<i>Spiniferites cf. pachydermus</i> (Rossignol) Reid, 1974	<i>Gonyaulax ellegaardiae</i> Mertens et al., 2015
		<i>Spiniferites ramosus</i> (Ehrenberg) Loeblich et Loeblich, 1966	<i>Gonyaulax spinifera</i> complex
Goniodomaceae	Cyst of <i>Alexandrium catenella</i>	<i>Alexandrium catenella</i> (Lebour) Balech, 1995	
Gymnodiniaceae	Cyst of <i>Pseudocochlodinium profundisulcus</i> Hu et al., 2021	<i>Pseudocochlodinium profundisulcus</i> Hu et al., 2021	
	Cyst of <i>Cochlodinium polykrikoides</i> sensu Li et al., 2015	<i>Cochlodinium polykrikoides</i> Margalef (1961)	
Peridiniaceae	Cyst of <i>Pentapharsodinium dalei</i>	<i>Pentapharsodinium dalei</i> Indelicato et Loeblich III, 1986	

TABLE 3 List of heterotrophic dinocyst taxa (theca- and cyst-based names) recorded for SMG in this study.

Family/Subfamily		Cyst-based name (paleontological)	Theca-based name (biological)
Polykrikaceae		Cyst of <i>Polykrikos kofoidii/schwartzii</i> complex	<i>Polykrikos kofoidii</i> (Chatton, 1914)/ <i>schwartzii</i> (Bütschli, 1873)
Protopteridimacae	Protopteridimioideae	<i>Brigantedinium cariacense</i> (Wall) Lentin et Williams, 1993	<i>Protopteridinium avellana</i> (Meunier) Balech, 1974
		Cyst of <i>Archaepertidinium minutum</i>	<i>Archaepertidinium minutum</i> Yamaguchi et al., 2011
		Cyst of <i>Protopteridinium americanum</i>	<i>Protopteridinium americanum</i> (Gran et Braarud) Balech, 1974
		Cyst of <i>Protopteridinium excentricum</i>	<i>Protopteridinium excentricum</i> (Paulsen) Balech, 1974
		Cyst of <i>Protopteridinium nudum</i>	<i>Protopteridinium nudum</i> (Meunier) Balech, 1974
		Cyst of <i>Protopteridinium stellatum</i>	<i>Protopteridinium stellatum</i> Wall (in Wall et Dale, 1968) Head (<i>comb. nov.</i>) in Rochon et al. (1999)
		<i>Echinidinium delicatum</i> (Zonneveld) Head 2003	unknown
		<i>Lejeunecysta marieae</i> Harland (in Harland et al., 1991) ex Lentin et Williams, 1993	<i>Protopteridinium</i> sp.
		<i>Quinquescuspis concreta</i> (Reid) Harland, 1977	<i>Protopteridinium leonis</i> (Pavillard) Balech, 1974
		<i>Selenopemphix nephroides</i> (Benedek) Benedek et Sarjeant, 1981	<i>Protopteridinium subnerme</i> (Paulsen) Loeblich III, 1970
		<i>Selenopemphix quanta</i> (Bradford) Matsuoka, 1985	<i>Protopteridinium conicum</i> (Gran) Balech, 1974
		<i>Votadinium calvum</i> Reid, 1977	<i>Protopteridinium latidorsale</i> (Dangeard) Balech, 1974
		<i>Votadinium spinosum</i> Reid, 1977	<i>Protopteridinium claudicans</i> (Paulsen) Balech, 1974
	Diplopsalioideae	<i>Dubridinium caperatum</i> Reid, 1977	<i>Preperidinium meunieri</i> (Pavillard) Elbrächter, 1993

Due to the difficulty of identification (because of bad orientation or folding) some spherical, non-reticulate, pigmented cysts without spines or ornaments lacking any evidence of archeopyle were grouped as “round brown” (usual name in the literature belonging to Protopteridinoideae or Diplopsalioideae). It was established that the count of each sample would end when the sum excluding *O. centrocarpum* exceeds 300 dinocysts to allow the remaining dinocyst taxa to be represented in the sum. In this way the total dinocyst sum for the calculation of taxa percentages and absolute abundances ranged from 622 to 9,126 cysts. Tilia software of Grimm (1990) was used to create a diagram of relative frequencies.

3.3 Oceanographic variables and calculation of stability parameters

Four hydrographic transects (two at the northern and two at the southern portion of the gulf) (Figure 1C) were chosen to describe the vertical structure of the water column from the inner gulf to the adjacent shelf during the time of the sediment sampling. Stations from the cruises C and PP were used to create sections of temperature and salinity (T and S), representing a snapshot of the hydrological spring conditions in the gulf (Figures 2, 3).

Historical hydrographic data were retrieved from the Regional Base of Oceanographic Data (BaRDO, INIDEP, Argentina) (Baldoni, 2022). A total of 49 CTD profiles were obtained between 2000 and 2010 covering the SMG area (Figure 4A) during spring (October-

December), which is the most productive season herein (Williams et al., 2010, 2021). We combined the historical data with the hydrographic data measured in the C and PP cruises, in order to obtain a long-term average of the oceanographic conditions considering that the cyst record from the upper centimeter of surface sediments could represent 10 or more years (Matthiessen et al., 2005). For this long-term analysis we used the average of spring sea-surface temperature and salinity (SSTs and SSSs) of the top 20 m that is the sea-surface layer where the dinoflagellates inhabit (de Vernal et al., 2007). Despite their ability to move vertically with their flagella, their living depth is relatively shallow, especially in stratified marine environments, because they cannot migrate across the pycnocline that constitutes an important physical barrier (e.g. Jephson et al., 2011).

The temperature and salinity data obtained from the CTD profiles were used to calculate the potential density (σ_T) and the Brunt-Väisälä buoyancy frequency (N^2), a measure of the stability of a fluid to vertical displacements:

$$N^2 = -\frac{g}{\rho_0} \frac{\partial \rho}{\partial z}$$

where g is gravity, ρ is the water density and Z the water column depth.

Calculations were made using the functions `swnSigmaTheta` and `swN2` of the package `oce` (Kelley et al., 2022) in R statistical software (R Development Core Team, 2021).

Sections of T and S during the time of sediment sampling (Figures 2, 3) and maps of long-term average of SSTs, SSSs, and

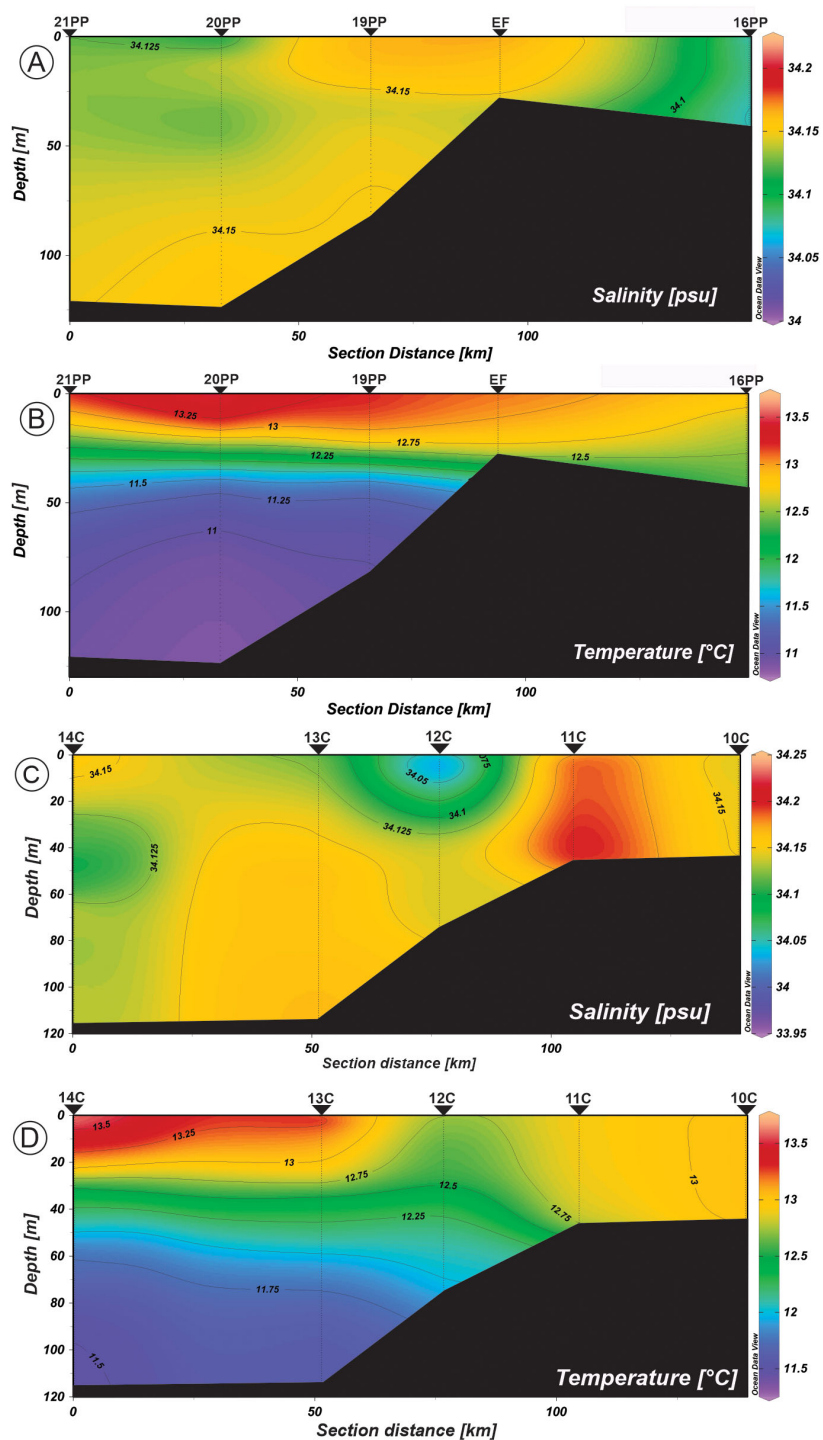


FIGURE 2 Salinity and temperature distribution profiles in the water column from the northern sections: (A, B) Transect I (Primavera Patagónica cruise, Nov. 2013). (C, D) Transect II (CONCACEN cruise, Nov. 2009).

maximum value of Brunt-Väisälä frequencies of the upper 20 m (B-V f) were displayed (Figures 4A-D) using the Ocean Data View Software (ODV-version 5.4.0, Schlitzer, 2021).

Nit-s comprised the contribution (in μM) from nitrates and nitrites for spring, and the surface values closest to each sampling stations, were selected from the map of Williams et al. (2001),

calculating the unknown value by linear interpolation taking into account the difference between the known data and the distance between the stations. These values corresponded to a sampling conducted in October 2009 (GSM-VI-09 Cruise G/C Río Paraná) and no other nutrient records were available for the spring of the gulf.

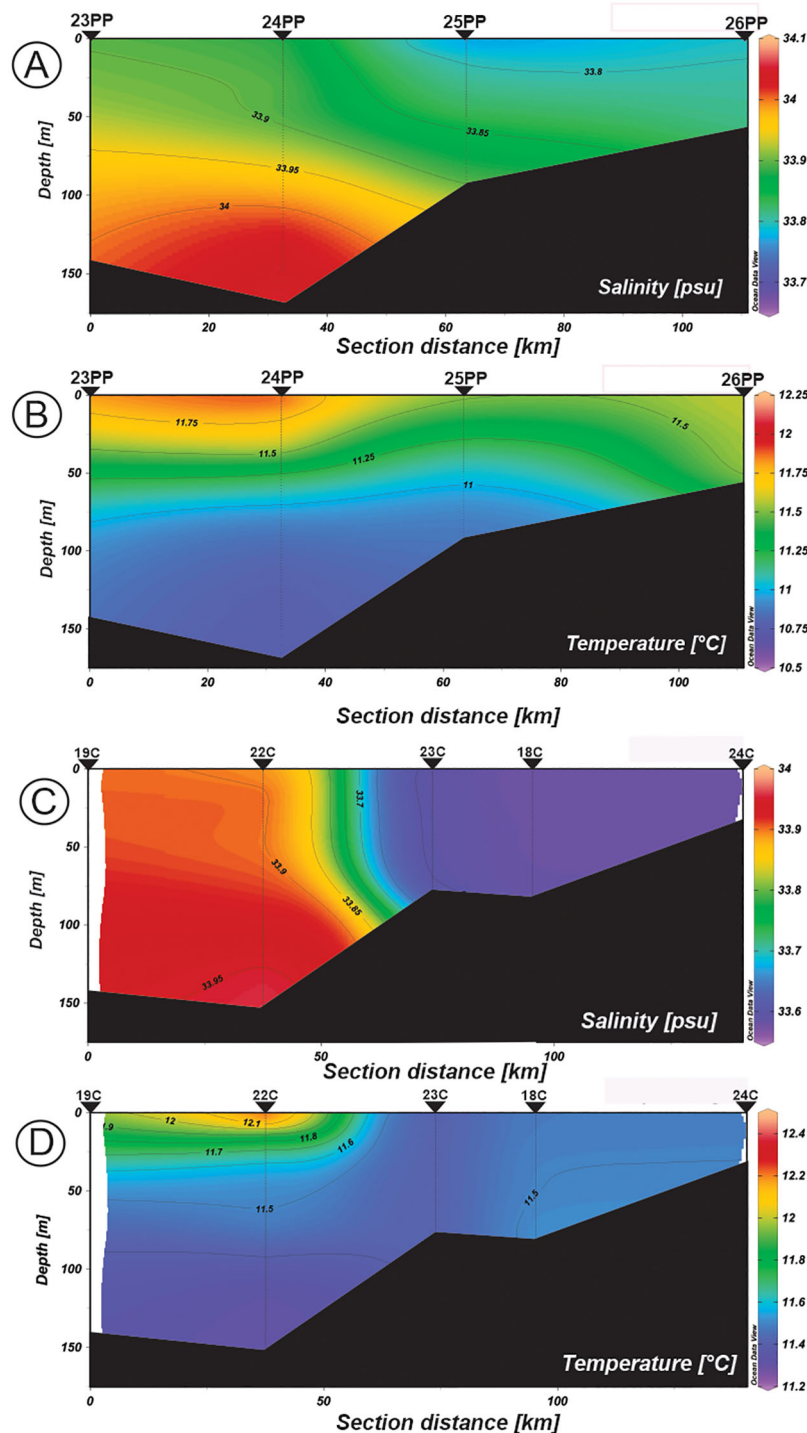


FIGURE 3 Salinity and temperature distribution profiles in the water column from the northern sections: (A, B) Transect III (Primavera Patagónica cruise, Nov. 2013). (C, D) Transect IV (CONCACEN cruise, Nov. 2009).

3.4 Grain size

Grain size analysis was conducted using a Mastersizer 2000 laser grain-size analyzer (Malvern Instruments, Malvern, UK) at the Laboratorio de Geología, Instituto Argentino de Oceanografía (IADO-CONICET). About 2–3 g of samples were treated with

35% (130 Vol.) hydrogen peroxide (H₂O₂) to eliminate organic matter. Subsequently, each one was homogenized and rinsed in 1000 mL of distilled water. The sample was dispersed for 10 min in an ultrasonic bath before measurement. The readings corresponded to the particle size by volume in percentages of the coarse sand (2.0–0.5 mm), medium sand (0.5–0.25 mm), fine sand (0.25–0.125 mm),

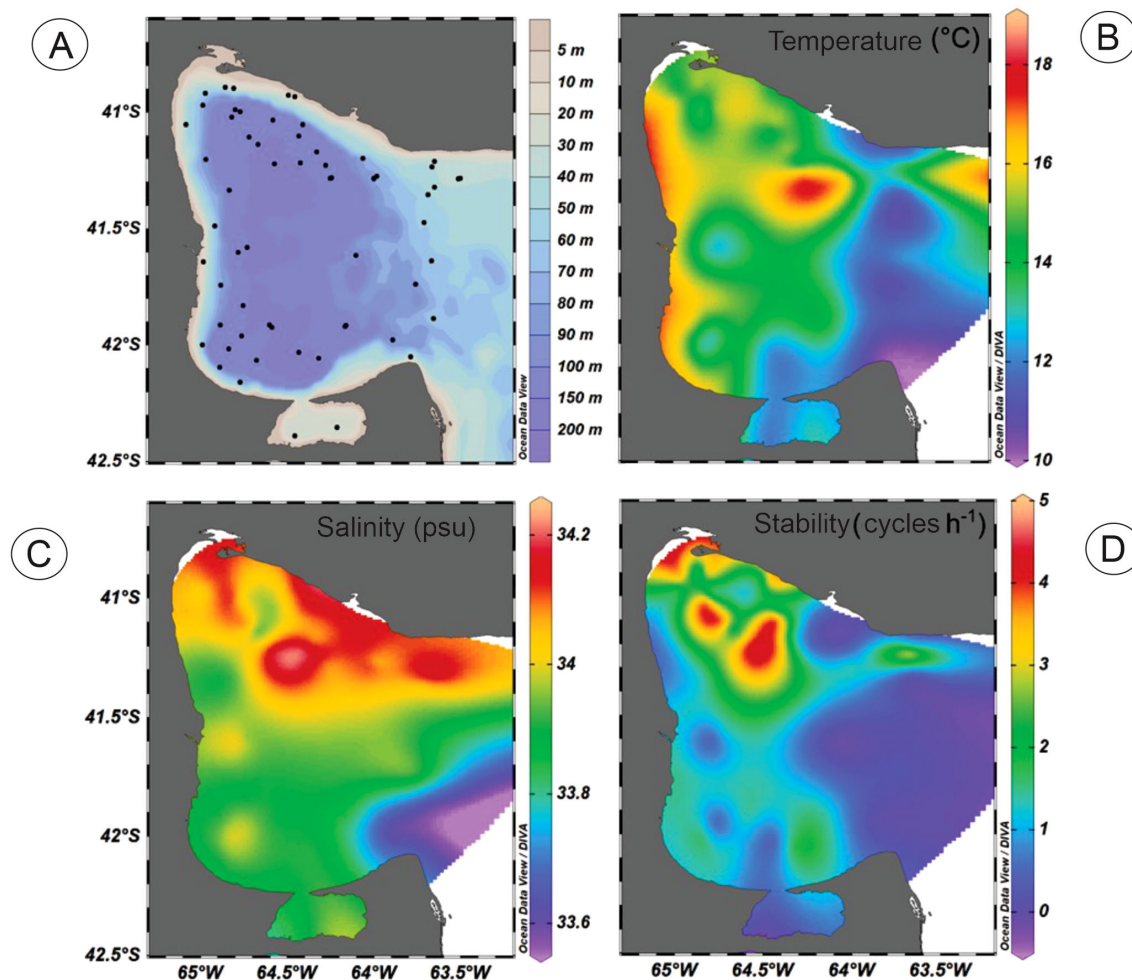


FIGURE 4

(A) Location of 49 CTD profiles obtained between 2000 and 2010 covering the SMG area. (B–D) Maps of the average of long-term oceanographic parameters at the surface water column (0–20 m) for spring months (October to December). (B) SSTs: spring sea- surface temperature ($^{\circ}\text{C}$). (C) SSSs: spring sea-surface salinity (psu). (D) B–V f: maximum value of Brunt–Väisälä stability (cycles h^{-1}).

very fine sand (0.125–0.063 mm), silt (0.063–0.0039) and clay (< 0.0039 mm) fractions (Wentworth, 1922). The classification of the collected sediments was made according to Shepard's diagram (Shepard, 1954), based on the proportions of sand, silt and clay sized particles (Figure 5, Table 1).

3.5 Statistical Analyses

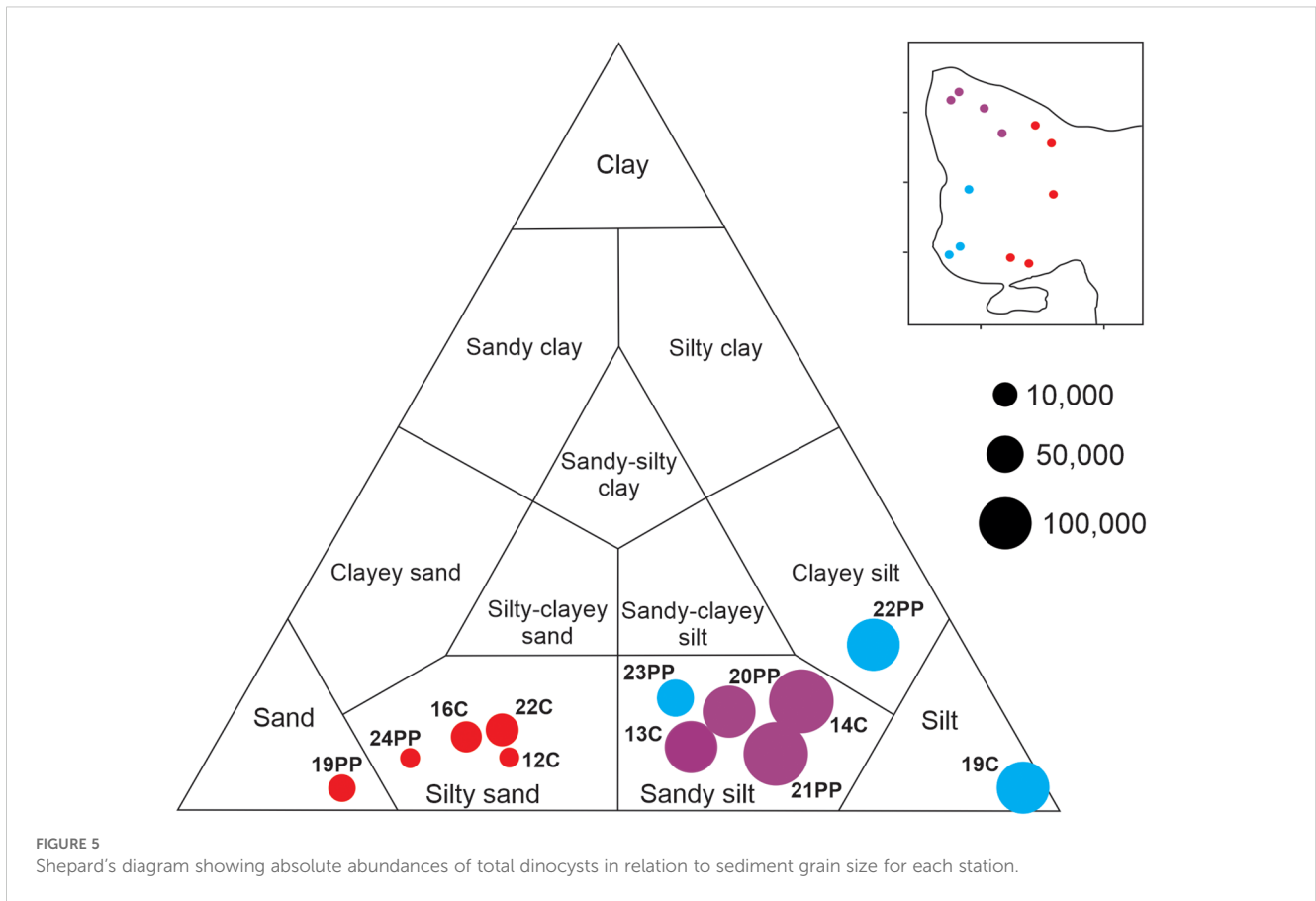
The PAST 4.11 statistical analysis software package (Hammer et al., 2001) was used to generate a trend analysis of the distribution of dinocyst assemblages. Principal Component Analysis (PCA) was applied in order to cluster the samples according to environmental conditions. Two environmental data set were used; the first comprised water column depth (Dth), silt proportion in the sediments (Silt) and surface concentration of nitrate in spring (Nit-s), and the data obtained at the time of sampling in each station: averaged SSTs and SSSs, and maximum values of B–V f (upper 20 m averaged) (Table 4). The second dataset included Dth,

Silt and Nit-s, and values interpolated from the long-term data for each sampling station: averaged SSTs and SSSs, and maximum values of B–V f (of the upper 20 m) (Table 4). We implemented a Detrended Correspondence Analysis (DCA) in order to identify the unimodal type function between dinocyst assemblages and environmental variables and to allow the further use of CCA (Canonical Correspondence Analysis). CCA were applied on the relative abundance standardized data $((x-x_{\text{mean}})/\text{SD})$ and were used to determine which environmental parameters explain most of the variance in the distribution of each dinocyst species.

4 Results

4.1 Composition and abundance of dinocyst assemblages

The number of taxa for an individual site (species richness) ranged from 14 to 25, with an average of 19 (Table 5). Dinocyst populations



were characterized by the dominance (in relative and absolute abundances) of phototrophic species which formed 82.98 to 95.95% of the total dinocysts (Figure 6). The absolute abundances of phototrophic cysts were in the range of 3,306 to 183,421 cysts g⁻¹ wet sediment (Table 5, Figures 7A, B). A total of 14 phototrophic taxa

were recognized (Table 2, Figure 8). *Operculodinium centrocarpum* (55-90.2%), *Spiniferites ramosus* (1.1-11.6%), *S. mirabilis* (0.5-2.4%), *Spiniferites* spp. (0.2-7.4%), cyst of *Alexandrium catenella* (0.2-4.3%) and cyst of *Cochlodinium polykrikoides* (0.2-1.5%) were present at all stations. *Pentapharsodinium dalei* (0.1-1.7%) was recorded in 5

TABLE 4 PCA and CCA environmental parameters: water depth (Dth), silt proportion (Silt), surface concentration of nitrate in spring (Nit-s), SSSs, SSTs and B-V f (during sampling) and SSSs, SSTs and B-V f (*long-term analysis).

St	Depth (m)	Silt (%)	Nit-s (µM)	SSTs (°C)	SSSs (psu)	B-V f (cycles h ⁻¹)	SSTs* (°C)	SSSs* (psu)	B-V f * (cycles h ⁻¹)
14C	129	62	1.9	13.45	34.15	1.26	13.5	34.1	1.8
21PP	131	54	1.9	13.38	34.12	4.60	13.5	34.1	3.8
20PP	133	54	1.9	13.58	34.05	4.84	13.8	34.05	3.9
13C	125	52	1.9	13.34	34.15	1.22	14.5	34.15	1.6
22PP	162	65	1	12.73	33.95	1.20	13	34.05	1
19C	149	98	0.8	11.49	33.58	0.008	13	34	0.4
23PP	127	47	0.6	12.73	34	1.85	13	34	1.5
19PP	86	16	1.2	13.37	34.15	0.0003	14	34.15	0.3
12C	83	33	1.8	12.47	33.99	0.735	16	34.05	1
16C	103	28	4.4	12.91	34	0.155	13.5	33.98	0.1
24PP	182	21	2.2	12.06	33.91	0.199	12	33.95	0.3
22C	157	31	2.8	13.07	33.95	0.146	12	33.95	1.4

TABLE 5 Species richness, relative (%) and absolute abundances (cysts g⁻¹ wet sediment) of phototrophic (P), heterotrophic (H), total (T), and *A. catenella* cysts for each sampling station.

Group	St	Species richness	Dinocyst relative abundances		Dinocyst absolute abundances			
			P	H	P	H	T	<i>A. catenella</i>
I NW N Zone	14C	25	95.37	4.63	166,618	8,088	174,706	2,426
	21PP	18	94.57	4.43	183,421	10,526	193,947	5,263
	20PP	14	95.84	4.16	113,882	4,941	118,823	4,882
	13C	19	95.95	4.05	123,414	5,207	128,621	310
II SW – S Zone	22PP	18	94.96	5.04	100,333	5,333	105,666	4,095
	19C	23	93.78	6.22	91,000	6,033	97,033	4,133
	23PP	15	95.63	4.37	48,494	2,205	50,699	1,888
III Mouth Zone	19PP	20	92.76	7.24	15,027	1,173	16,200	545
	12C	19	83.7	16.3	3,306	644	3,950	169
	16C	24	82.98	17.02	19,587	4,079	23,666	143
	24PP	16	87.62	12.38	4,542	642	5,184	134
	22C	24	94.08	5.92	28,452	1,790	30,242	807

stations. *Spiniferites bulloideus*, *S. belerius*, *S. cf. pachydermus*, *S. lazus*, *S. ludhamensis*, *Achomosphaera* sp. and cyst of *Pseudocochlodinium profundisulcus* presented low frequencies (< 1%) in few stations (Figure 6).

The absolute abundances of heterotrophic cysts were in the range of 642 to 10,526 cysts g⁻¹ wet sediment (Table 5, Figures 7A, B). Within the heterotrophic dinocysts we found 16 taxa (Table 3, Figure 9). Cysts of *Protoperidinium nudum* (0.3–5.8%),

Archaerperidinium minutum (0.3–3.8%) and *Polykrikos kofoidii/schwartzii* (0.7–5.4%), cysts grouped as “round brown” (0.3–3.5%), *Votadinium spinosum* (0.1–1%) and *Dubridinium caperatum* (0–4.1%) were the main heterotrophs. *Votadinium calvum*, *Quinquecuspis concreta*, cysts of *Protoperidinium americanum*, *P. stellatum* and *P. excentricum*, *Lejeunecysta mariae*, *Echinidinium delicatum*, *Selenopemphix nephroides* and *S. quanta* were present in few stations and in low numbers (< 1%) (Figure 6).

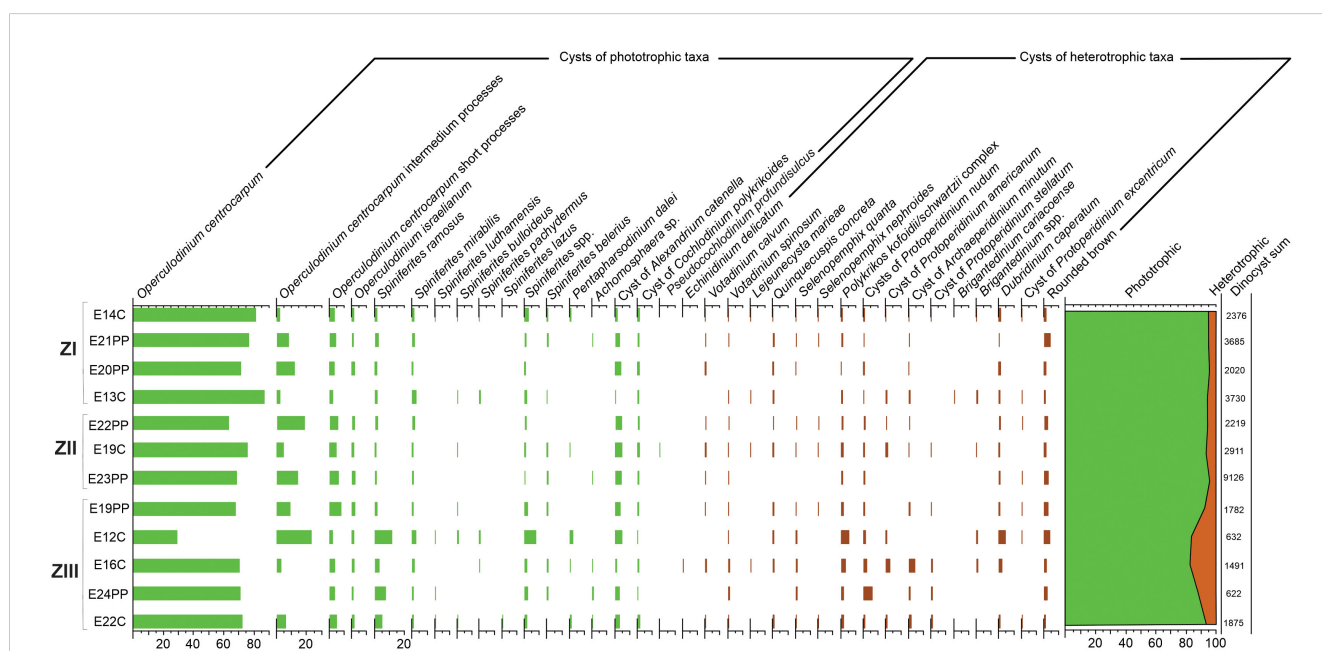
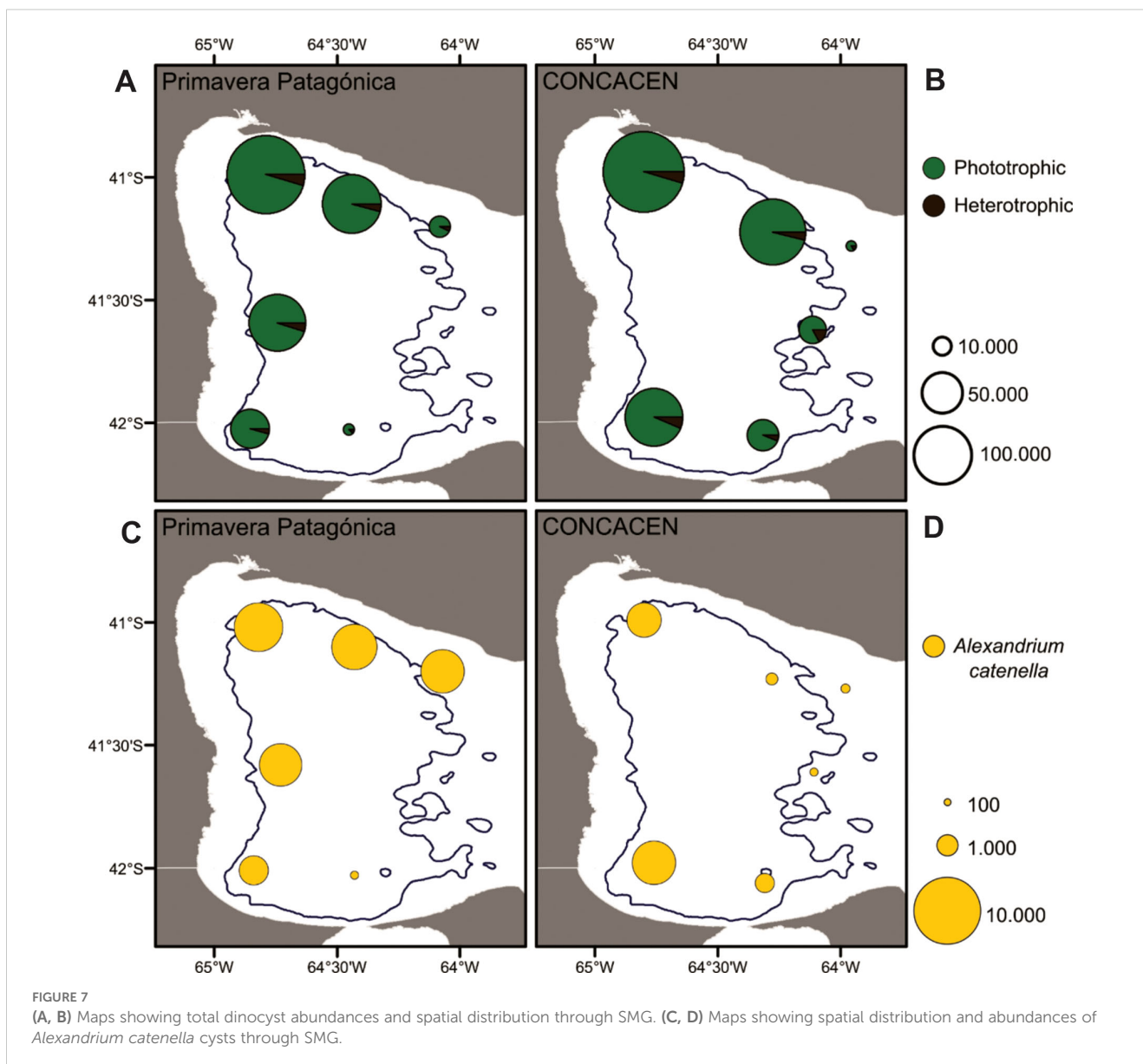


FIGURE 6 Relative dinocyst abundances (%) for the 12 surface samples in Zones I (ZI), II (ZII) and III (ZIII) of SMG.



4.2 Oceanographic conditions at the time of sampling

Temperature showed a clear stratification with values that range from 11.0 to 13.5°C in the north (Transects I and II, [Figures 2B, D](#)) and a weaker vertical structure from 10.75 to 12.4°C in the south (Transects III and IV, [Figures 3B, D](#)), reaching the highest values within the shallower 30 m. Salinity of the gulf varied between 34.12 and 34.15 in the inner northern area of the gulf ([Figures 2A, C](#)), while in the southern sections it ranged from 33.6 to 34.1 ([Figures 3A, C](#)). The salinity variation of 33.6 to 33.9 along the transect IV reflected the intrusion of less saline shelf-water through the southern sector of the mouth of the SMG ([Figure 3C](#)). The maximum values of the B-V f for the upper 20 m of the water column were greater at the northern stations (4.60 cycles h^{-1} for 21PP and 4.84 cycles h^{-1} for 20PP) ([Table 4](#)).

4.3 Average of long-term hydrographic conditions

A compilation of spring hydrographic data was used to assess the spatial distribution of the SSTs and SSSs contextualizing the cyst record within the long-term environmental conditions. The distribution of the surface temperature (top 20 m averaged) showed the highest values in the NW-N and shallow coastal areas of the gulf, while it decreased towards the east where it reached the lowest values above its mouth ([Figure 4B](#)). A general decrease from the coast to the adjacent shelf, while a maximum in surface salinity ([Figure 4C](#)) was observed at the northern portion of the gulf. As a result, the north of the gulf is more stratified than the south, as disclosed by the higher stability values ([Figure 4D](#)).

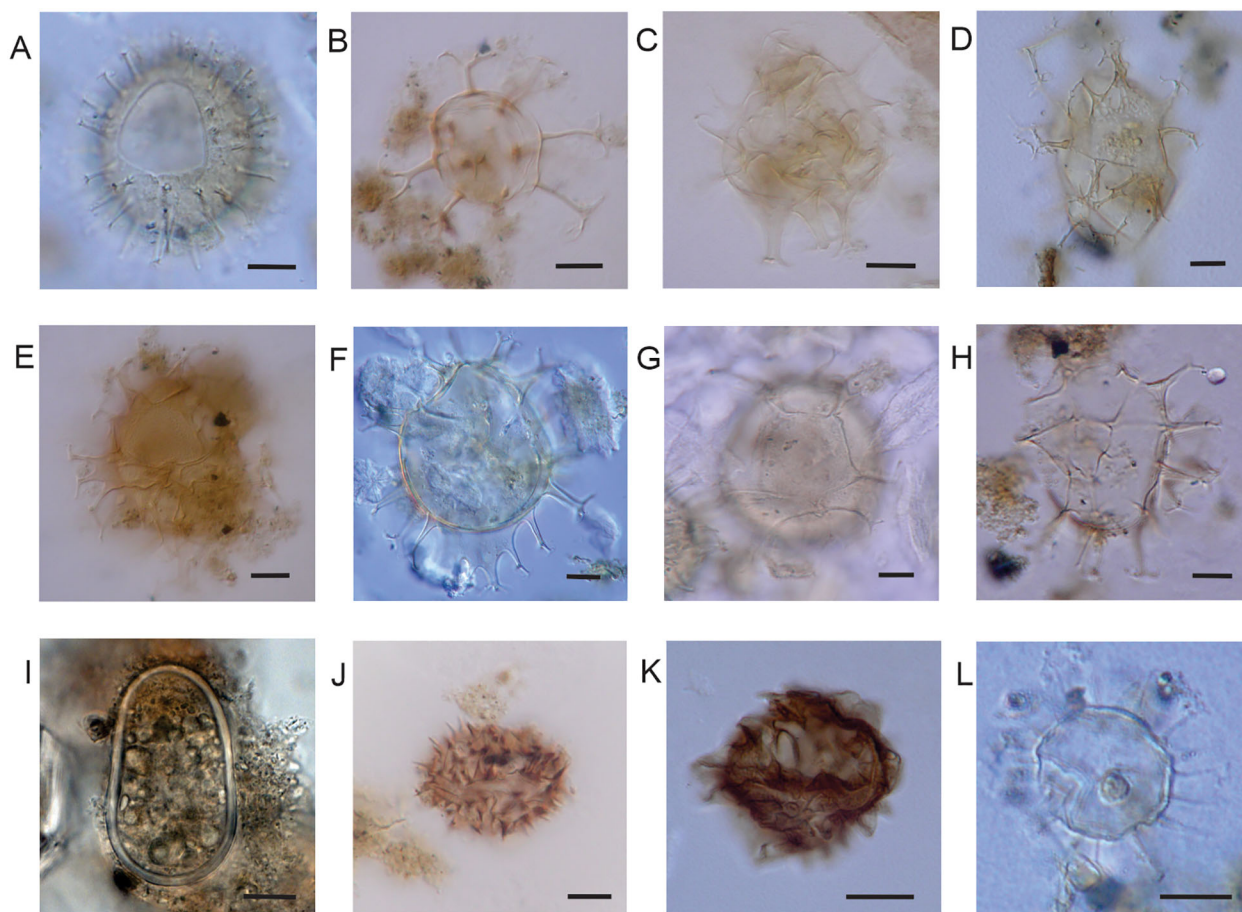


FIGURE 8

Phototrophic dinocysts of surface sediments of SMG (LPUNS slides and England Finder coordinates). (A) *Operculodinium centrocarpum* (St16C K30/4), with "normal" long processes. (B) *Achomosphaera* sp. (St24PP S25/3). (C) *Spiniferites bulloideus* (St19C J42/2). (D) *Spiniferites lazus* (St22C S37/4), surface view showing the fenestrate processes. (E) *Spiniferites ludhamensis* (St24PP M 22/3). (F) *Spiniferites mirabilis* (St13C O60/2). (G) *Spiniferites* cf. *pachydermus* (St13C Q67/1). (H) *Spiniferites ramosus* (St24PP G26/0). (I) Cyst of *Alexandrium catenella* (St24PP A37/3). (J) Cyst of *Cochlodinium polykrikoides* (St23PP C33/4). (K) Cyst of *Pseudocochlodinium profundisulcus* (St19C Q42/1). (L) Cyst of *Pentaparsodinium dalei* (St22C F33/0). Scale bars = 10 μm .

4.4 Grain size of bottom sediments

The size of the cyst-bearing sediments was dominated by sands and silts with some clay component (Table 1). The Shepard diagram (Figure 5) allowed us to classify them into two main textures: silty sands and sandy silts. The sediments of samples collected from more distant sectors of the gulf mouth (Figure 1B; 14C, 21PP, 20PP, 13C, 23PP) were sandy silts with depths between 125 and 133 m. Samples 22PP and 19C were composed of clayey silt and silt respectively, where the grab reached higher depths (162 and 149 m) in inner sectors of the basin. Near the gulf sill (Figure 1B; 12C, 16C, 22C) with depths ranging from 83 and 157 m, sediments were coarser, represented by silty sands. Sample 19PP, also located near the gulf mouth and proximate to the northern coast, turned out to be distinctly sandy. Despite the greatest depth of sample 24PP (182 m), it was composed mainly of sand (71%; Table 1) linked to its position near the mouth of San José Gulf (SJsG). The textural distribution of the sediments analyzed here is consistent with the previous record of Mouzo and Paterlini (2017).

4.5 Analyses and relationship between cyst distribution and environmental parameters

PCA have been performed on selected parameters (Table 4) in order to cluster the samples according to the environmental conditions, coming from both: the time of sediment sampling and long-term measurements. The first two component axes together explained 70.24% of the variation of environmental conditions using SSTs, SSSs and B-V f obtained from data at the time of sampling (Table 6A), and explained 68.10% of the variation of environmental conditions using SSTs, SSSs and B-V f of long-term analysis (Table 6B). The PCA plots (Figures 10A, B) showed the grouping of samples in relation to three different water masses and grain size sediment. SSTs, SSSs and B-V f were positively correlated. Zone I was located in the NW-N of the gulf (Figure 1B) where SSTs (13.34–13.58°C), SSSs (34.05–34.15) and B-V f (1.22 to 4.84 cycles h^{-1}) reached the highest values. The surface concentration of nitrate in spring (Nit-s) was medium (1.9 μM) and the sediments were sandy

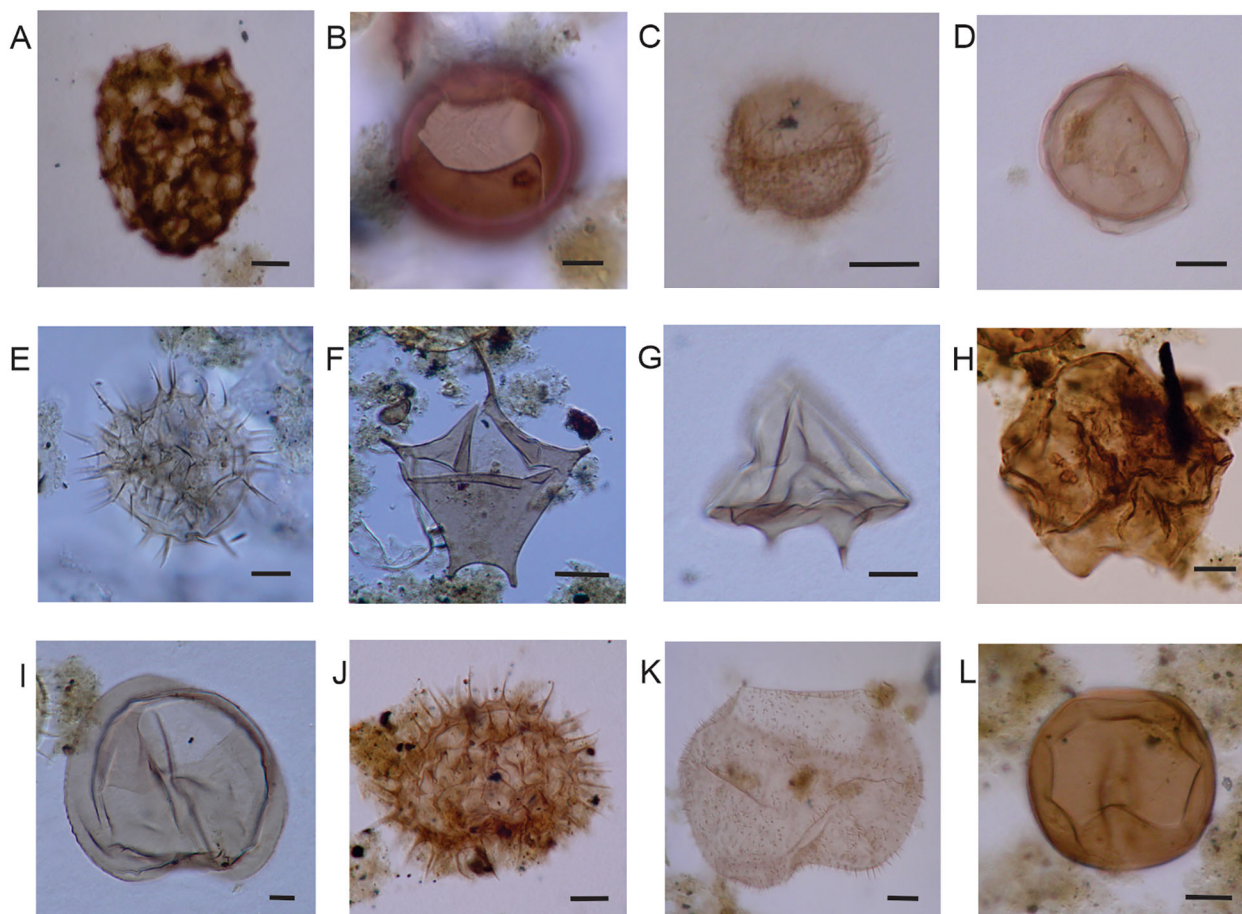


FIGURE 9

Heterotrophic dinocysts of surface sediments of SMG (LPUNS slides and England Finder coordinates). (A) Cyst of *Polykrikos kofoidii* (St22PP O34/0). (B) *Brigantedinium cariacense* (St13C E64/4). (C) Cyst of *Archaeoperidinium minutum* (St23PP E23/2). (D) Cyst of *Protoperidinium americanum* (St19C M44/3). (E) Cyst of *Protoperidinium nudum* (St16C Y28/2). (F) Cyst of *Protoperidinium stellatum* (St19PP U31/2). (G) *Lejeunecysta mariae* (St14C P24/4). (H) *Quinquecuspis concreta* (St13C G51/0). (I) *Selenopemphix nephroides* (St14C P41/4). (J) *Selenopemphix quanta* (St24PP Q24/3). (K) *Votadinium spinosum* (St24PP O29/0). (L) Cyst of *Protoperidinium excentricum* (St22PP Y39/3). Scale bars = 10 μm .

silt. Zone II was composed of samples located in SW-S of the gulf (Figure 1B) characterized by lower values of SSTs (11.49–12.73°C), a wide range of SSSs (33.58–34) and low B-V f (0.008–1.85 cycles h^{-1}). Nit-s was low and ranged from 0.6 to 1 μM and the sediments were mainly silt. Zone III was situated in the mouth of the gulf (Figure 1B) with medium values of SSTs (12.06–13.37°C) and SSSs (33.91–34.15), the lowest values of B-V f (0.0003–0.735 cycles h^{-1}) and the highest values of Nit-s (up to 4.4 μM). The sediments were mainly sand.

The CCA analyses showed that the two axes together explain 86.68% of the canonical variance in the dataset of sampling day (Table 7A) and together explain 95.35% of the canonical variance for the long-term dataset (Table 7B). Surface concentration of nitrate in spring, water-depth and Brunt-Väisälä frequency seem to be the environmental parameters that played an important role in the dinocyst species ordination. When the long-term values were considered, the sea-surface temperature of spring (SSTs) appeared as one of the factors ordering some phototrophic taxa such as *Spiniferites bulloideus*, *S. cf. pachydermus* and *Pentapharsodinium dalei*. Most heterotrophic taxa (such as *V. spinosum*, *Selenopemphix*

quanta, cyst of *Protoperidinium nudum*, cyst of *P. americanum*, cyst of *Archaeoperidinium minutum* and cyst of *P. stellatum*) showed a strong correlation with nitrate values (Nit-s) (Figures 11A, B).

5 Discussion

5.1 Inner area of the gulf

The abundances of dinocysts recorded for the NW-N (Zone I) and SW-S (Zone II) of San Matías Gulf (Northern Patagonia) reach values as high as 193,947 and 105,666 cysts g^{-1} wet sediment, respectively (see Table 5). Comparable amounts of dinocysts in surface sediments were registered in the data base of the Northern Atlantic Ocean (> 100,000 cysts cm^{-3}) along coastal sites such as inland seas and estuaries whereas the lowest densities (< 100 cysts cm^{-3}) characterize offshore sites (de Vernal et al., 2005, 2007). In the Argentine Sea, within San Jorge Gulf (central Patagonia), Faye et al. (2018) have documented abundances of 45,848 cysts g^{-1} dry sediment, and near its mouth, Krock et al. (2015) reported up to

TABLE 6 PCA eigenvalues, variance and correlation matrix, in relation to six principal components.

(A) At the time of sampling analysis						
	PC1	PC2	PC3	PC4	PC5	PC6
Eigenvalues	2.66537	1.54914	0.863178	0.550593	0.311075	0.0606507
Variance %	44.423	25.819	14.386	9.1765	5.1846	1.0108
B-V f	0.22285	0.64826	0.26915	0.22874	-0.63414	0.056589
Nit-s	0.24859	-0.47099	0.58457	0.59315	0.079418	0.1285
SSTs	0.54935	0.25653	0.10631	-0.044808	0.42517	-0.66206
SSSs	0.57349	0.12082	-0.0407	-0.29281	0.26518	0.70625
Silt	-0.36904	0.50633	-0.061707	0.49799	0.55972	0.2058
Dth	-0.34881	0.14547	0.75437	-0.51	0.16488	0.028472
(B) Long term analysis						
	PC1	PC2	PC3	PC4	PC5	PC6
Eigenvalues	2.33418	1.75034	0.911529	0.531718	0.324823	0.147413
Variance %	38.903	29.172	15.192	8.862	5.4137	2.4569
B-V f*	0.1474	0.37976	0.85144	-0.098471	-0.30256	-0.088732
Nit-s	-0.091902	-0.57625	0.49316	0.45539	0.45236	0.065363
SSTs*	0.6004	-0.05745	-0.074769	0.32194	-0.28996	0.66551
SSSs*	0.53388	0.23053	0.025926	-0.35781	0.72945	0.03208
Silt	-0.063233	0.62392	-0.1243	0.72125	0.21428	-0.1586
Dth	-0.56597	0.27929	0.1007	-0.17617	0.20429	0.72025

(A) SSTs, SSSs and B-V f (during sampling). (B) SSTs, SSSs and B-V f (*long-term analysis).

17,000 cysts g^{-1} wet sediment, with maxima in finer grain-sized sediments. Nevertheless, they are still low values when compared with the dinocyst densities herein presented which could be due to the more restricted conditions of the semi-enclosed SMG.

According to the data obtained in this study the water column in the NW-N region (Zone I) was stable (as suggested by higher B-V f values) and stratification was driven by temperature vertical differences in spring (see Figure 2, Transects I and II). Precisely, in this zone the dinocyst abundances were the highest of the gulf (> 118,000 cysts g^{-1} wet sediment), largely represented by the phototrophic group. Since the vertical fluxes of cysts depend on the production in the upper water column, the dinocyst record is mostly determined by the characteristics of the surface water (Anderson et al., 2005; de Vernal et al., 2007). In particular, a stratified water column enhances the proliferation of phototrophic dinoflagellates, which unlike diatoms have an active behavior owing to their flagella thus being able to actively migrate within the water column (Smayda, 1997). The enclosed Zone I displays a bimodal cycle of phytoplankton biomass with maxima in spring and in autumn as shown by the Chl-a data (Williams et al., 2021).

Thus, the elevated cyst densities in Zone I evidence successive annual and interannual proliferations of phototrophic dinoflagellates, given that the upper centimeter of surface sediments may represent ten or more years (Matthiessen et al., 2005; Matsuoka and Fukuyo, 2000). Likewise, the integration of

several years of productivity in bottom sediments was considered to interpret differences of dinocyst records between sediment-traps and surficial sediments, and to explain augments of dinocyst abundances in annually sampled sites from the Arctic fjords (Howe et al., 2010; Richerol et al., 2012).

The signal in dinocyst assemblages of a long-term succession of dinoflagellate blooms favored by the surface-water characteristics in the Zone I is further influenced by the restricted water exchange with the open ocean due to the internal water circulation of SMG. The bathymetric restriction originated by the isolation from the shelf through a sill (Mouzo and Paterlini, 2017) and the system of cyclonic gyre located in the northern and a less defined closed circulation pattern in the southern gulf (Tonini et al., 2013) could be acting as a trap holding the fine sediments and dinocysts inside the basin. Similarly, this isolation of the northern SMG in spring-summer seems to be important in the larval retention and persistence of shellfish population (Amoroso et al., 2011). The reduced horizontal transport to the open ocean may prolong the residence time of cysts in suspension, increasing the probability of their eventual deposition within the basin, particularly in fine sediment areas. Moreover, within the Zone I the highest cyst densities occur at deep stations (> 120 m) where the fine fractions of sediments (silt specifically, < 63 μm) are predominant (> 52%). As it is known, the quite similar hydrodynamic behavior of the dinocysts to the silt particles, due to their size, allows its deposition

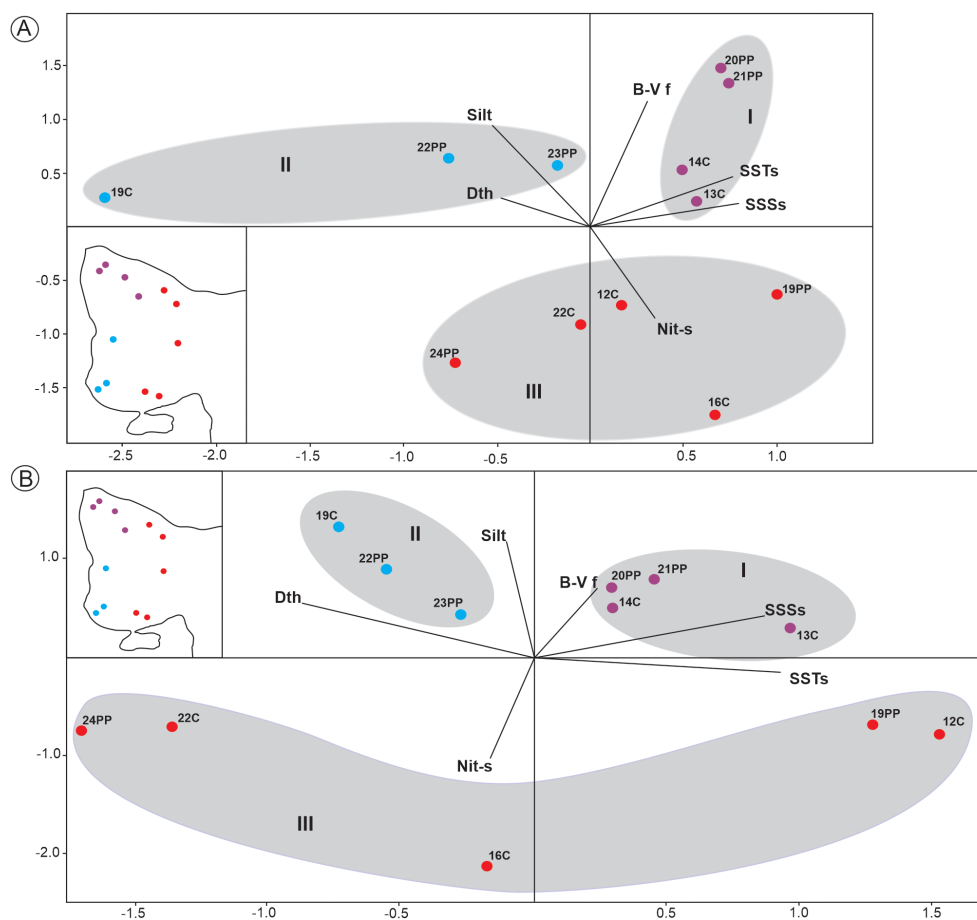


FIGURE 10
PCA analyses of samples based on environmental parameters: **(A)** SSTS, SSSs and B-V f at the time of sediment sampling, Dth, Silt and Nit-s. **(B)** Long-term SSTS, SSSs and B-V f, Dth, Silt and Nit-s.

in fine sediments (e.g. Dale, 1976). In this regard, the seafloor circulation was inferred from the sediment's grain-size distribution, identifying a fine-sediment deposition area in the southernmost part of the gulf (Hernández-Moresino et al., 2019). Furthermore, the zonal front present in the region could contribute to a secondary vertical circulation (Acha et al., 2004) that may enhance the sinking of organic matter and cysts, favoring their accumulation in deep areas. Even though the cyst densities are lower in S-SW of the gulf (Zone II), they still show high values which could be also the result of conditions that favor the development of phototrophic dinoflagellates, mainly a water column that reaches some stabilization in deeper sites during spring (see Figures 3B, D, Transects III y IV) and summer, and the incorporation of several years of cyst fluxes in sediments dominated by silt (> 47%).

The seasonal stability of the water column, the high phytoplankton productivity, and the low-energy conditions favor the accumulation of phototrophic dinocysts in fine sediments, making the SMG an ideal environment for the settlement of sedimentary seed banks. This is particularly evident in Zones I and II, where dinocysts can remain preserved for long periods, representing a multi-year sedimentary record. The seed banks are key reservoirs for the regeneration of dinoflagellate populations,

especially if they are potentially toxic, as they enable the release of vegetative cells contributing to the development of new blooms (Smayda, 2002).

5.2 Unrestricted area of the gulf

The coarser grain-size of the sediments in the Zone III (with > 57% of sand and less than 33% of silt) might explain the decrease of the dinocyst abundances (< 30,250 cysts g^{-1}) in agreement with the higher environmental energy near the mouths of SMG and SJsG (Mouzo and Paterlini, 2017). This Zone III is distinguished by higher relative frequencies (up to 17%) of heterotrophic cyst species (Figure 6). Dinocyst assemblages in sediments reflect the nutrient concentrations of sea surface water because the increase of heterotrophic cyst occurs with an increase of primary productivity that promotes the availability of prey such as diatoms, tintinnids and other dinoflagellates (e.g. Zonneveld et al., 2001; Dale et al., 2002; Radi and de Vernal, 2004). Congruently, diatom prevalence in the phytoplankton abundance of this zone was recorded by Carreto and Verona (1974) in agreement with the lower B-V f (Figure 4D) that point an unstable water column encouraging the diatom dominance. Also, cysts of *Echinidinium*

TABLE 7 CCA eigenvalues, variance and correlation matrix between environmental parameters and the first four ordination axes.

(A) At the time of sampling analysis				
	Axis 1	Axis 2	Axis 3	Axis 4
Eigenvalues	0.057709	0.023668	0.01066	0.0018429
Variance %	61.47	25.21	11.35	1.963
B-V f	-0.41271	-0.180336	-0.105046	-0.456763
Nit-s	0.509733	0.45079	-0.277117	0.152078
SSTs	-0.309972	-0.0250087	-0.535836	0.110893
SSSs	-0.105304	-0.0773877	-0.293042	-0.0306401
Dth	-0.405344	0.490348	0.359874	-0.0315323
(B) Long term analysis				
	Axis 1	Axis 2	Axis 3	Axis 4
Eigenvalues	0.047847	0.030619	0.003826	2.0127E-14
Variance %	58.14	37.21	4.649	2.446E-11
B-V f*	-0.418703	0.266885	-0.31042	0.0129923
Nit-s	0.538446	-0.466362	-0.16654	-0.0116876
SSTs*	0.511431	0.736185	0.0573091	-0.0626438
SSSs*	-0.230494	0.406786	-0.334761	0.570226
Dth	-0.473658	-0.462593	0.141184	-0.0710137

Bold variables are significant at the 5% significance level. (A) SSTs, SSSs and B-V f (during sampling). (B) SSTs, SSSs and B-V f (*long-term).

delicatium are present only in the Zone III (station 16C, mouth of SMG) where the values of spring nitrates are the highest of the gulf (up to 4.4 μM) (Williams et al., 2021). *E. delicatium*, was previously reported from vertically mixed and nutrient enriched areas, such as coastal bays in southern South Korea (Pospelova and Kim, 2010). This species, along with other heterotrophic dinocyst taxa (such as cysts of *Protoperidinium nudum*, *P. americanum*, *P. stellatum*, *Archaeperidinium minutum*) are aligned with the nitrate concentrations as depicted by the CCA.

Close to the mouth of the gulf, previous studies based on satellite images have shown mechanisms governing water exchange between the SJsG and the SMG (Amoroso and Gagliardini, 2010; Marmorino et al., 2017) that alter the horizontal distribution of nutrients and phytoplankton biomass (Williams et al., 2021) and consequently the deposition of dinocysts in the bottom sediments. At the mouth of the SMG (stations 19PP, 12C, 16C) and close to SJsG (stations 24PP and 22C) the instability of the water column and the increase of the energy in the depositional environments inferred from the coarse grain-sized sediments seems to be the drivers for the increase of the relative frequencies of heterotrophic dinocysts and the general decline of dinocyst densities.

5.3 Harmful species

Among cyst taxa the benthic phase of the potentially harmful species *Protoceratium reticulatum* (*O. centrocarpum*) is remarkably

dominant. High percentages of *O. centrocarpum* in modern dinocyst assemblages (up to 91%) have also been reported for coastal to open oceanic sites from the temperate to subpolar North Atlantic Ocean (Zonneveld et al., 2013). In the Argentine shelf, *P. reticulatum* have a wide distribution from 37 to 53°S (Balech, 1988; Akselman et al., 2015) which is in line with its occurrence in plankton samples of PP cruise at several stations of the continental shelf and the slope between 39 and 47°S; however, no *P. reticulatum* cells were detected in the SMG (Fabro et al., 2018). The mismatch between high relative values of *P. reticulatum* cysts and low values of their cells in plankton was also documented by Akselman et al. (2015) in two other sectors of the northern Argentinian shelf (EPEA: Permanent Station of Environmental Studies, at 38°28'S-57°41'W, and AUCFZ: Argentine-Uruguayan Common Fishing Zone, between 34°00' and 39°30'S). This discrepancy can be a result of the fact that cyst assemblages reflect an average of cysts produced by planktonic communities over time whereas plankton sampling means only a temporal and spatial snapshot (Matthiessen et al., 2005). This hypothesis is further supported by Ellegaard et al. (2003) who indicated that cultures of *P. reticulatum* were short lived and encysted quickly and spontaneously. Yessotoxins (YTXs) produced by *P. reticulatum* were detected from the plankton of the Argentine shelf near the slope (Fabro et al., 2018) and previously in San Jorge Gulf, where the YTX production was confirmed in strains of the isolated species (Akselman et al., 2015). Although no YTXs have been detected inside the SMG, the great abundances of *P. reticulatum* cysts in the gulf sediments can be considered a warning regarding the development of toxic events in the future.

The presence of ellipsoidal cysts of *A. catenella* in SMG sediments is of particular interest and concern since they can trigger the outbreak of recurrent blooms and resulting PSP (paralytic shellfish poisoning) incidents. The species is present at all stations with varying densities of 134 to 5,263 cysts g^{-1} wet sediment, exhibiting higher values in the inner gulf (Zones I and II, with exception of station 13C) and lower values in the mouth of the gulf (Zone III) (Figures 7C, D). In agreement with this widespread distribution of benthic cysts, plankton data from the PP cruise (Fabro et al., 2017) showed extensive distribution of cells inside the gulf and its mouth (stations 19PP, 20PP, 22PP, 23PP, and 24PP). However, the highest densities of *Alexandrium* cells and of toxin levels were measured in samples located in the frontal zone of the Valdés Peninsula (outer area of the gulf) (Carreto et al., 1986; Fabro et al., 2017). The sediment samples of the stations of the Valdés Peninsula front were composed only by coarse fractions (coarse sand, shell and gravel) and the dinocysts were absent, revealing an area of probably rapid cyst depletion (by transport). However, in the interior of the SMG there are significant densities of *A. catenella* cysts whose accumulation can be linked to the presence of fine sediments in the lower energy sectors. The fact that *Alexandrium* cysts survive in sediments as viable cysts (with a germination ability) from years to decades (Miyazono et al., 2012; Feifel et al., 2015) gives a particular relevance to this report indicating that the cyst deposited in the inner SMG could potentially act as a seed bank.

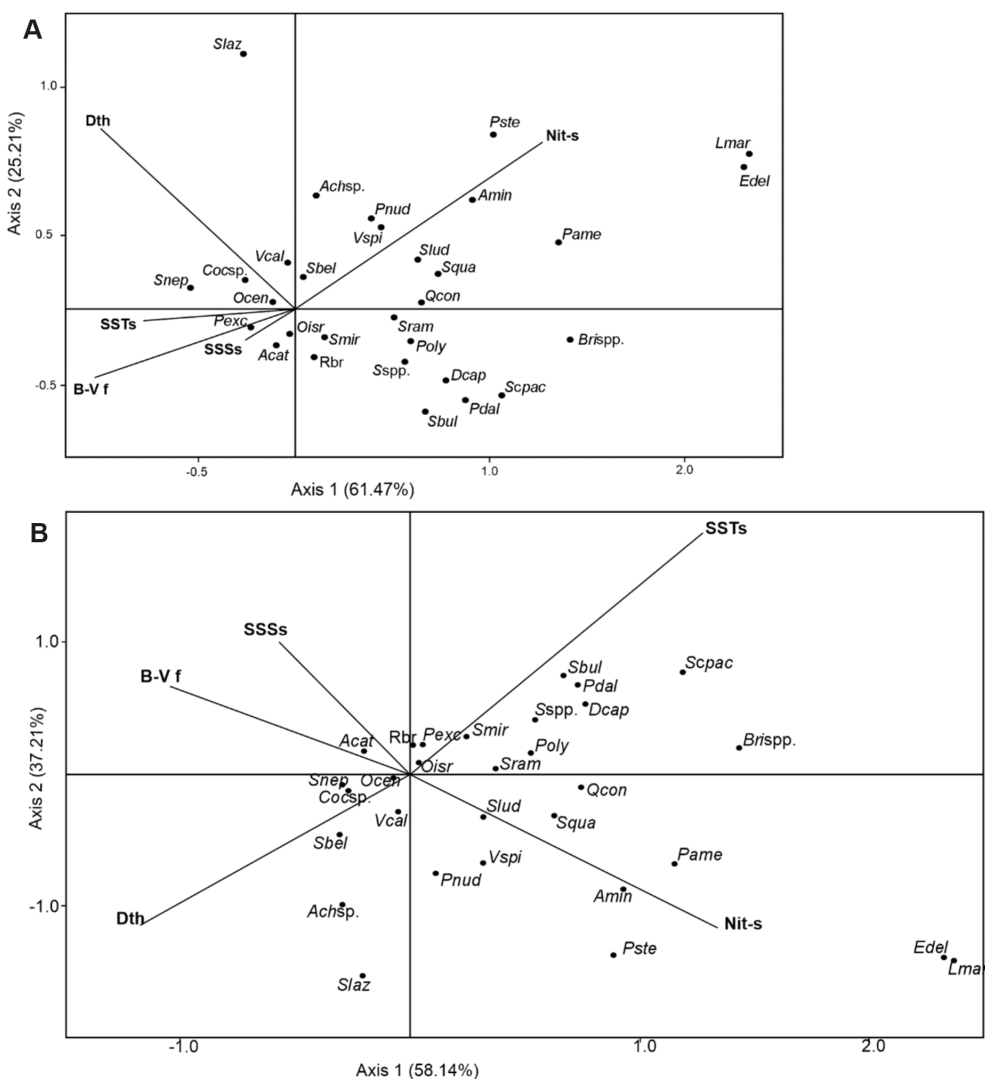


FIGURE 11
 Ordination diagrams generated from CCA. **(A)** Ordination of dinocyst taxa and environmental parameters (SSTS, SSSs and B-V f at the time of sediment sampling, Dth, Silt and Nit-s). **(B)** Ordination of dinocyst taxa and environmental parameters (long-term SSTS, SSSs and B-V f, Dth, Silt and Nit-s). Ocen: *Operculodinium centrocarpum*, Oisr: *Operculodinium israelianum*, Achsp: *Achomosphaera* sp., Sbel: *Spiniferites belerius*, Sbul: *S. bulloideus*, Slaz: *S. lazus*, Slud: *S. ludhamensis*, Smir: *S. mirabilis*, Scpac: *S. cf. pachydermus*, Sram: *S. ramosus*, Sspp: *Spiniferites* spp.; Acat: cyst of *Alexandrium catenella*, Cocsp: cyst of *Cochlodinium polykrioides*, Pdal: cyst of *Pentapharsodinium dalei*, Rbr: round brown; Poly: cyst of *Polykrikos kofoidii/schwartzii* complex, Brsp: *Brigantedinium* spp., Amin: cyst of *Archaeoperidinium minutum*, Dcap: *Dubridinium caperatum*, Pame: cyst of *Protoperidinium americanum*, Pexc: cyst of *P. excentricum*, Pnud: cyst of *P. nudum*, Pste: cyst of *P. stellatum*, Lmar: *Lejeunecysta mariae*, Qcon: *Quinquecupis concreta*, Snep: *Selenopemphix nephroides*, Squa: *S. quanta*, Vcal: *Votadinium calvum*, Vspi: *V. spinosum*, Edel: *Echinidinium delicatum*.

Two species of cysts attributed to *G. spinifera* complex (*Spiniferites mirabilis* and *S. ramosus*; see Table 2) were persistently present at all sampled sites. The *G. spinifera* complex presents a wide distribution in the phytoplankton of the Argentine Sea from 39 to 55°S. During the PP spring cruise their cells were detected only at one of the stations (station 19PP, northern mouth of the SMG), but they were present at the N, SW and mouth of SMG during a late summer cruise (march 2013) (Fabro et al., 2018). This fact could be related to the spatio-temporal progress of the motile stage with the warm season. *G. spinifera* has not been clearly associated with YTXs in the Argentine shelf (Akselman et al., 2015; Fabro et al., 2018). Recently, Gu et al. (2021) indicated that

the lack of YTX-production for strains of *G. spinifera* is consistent with the reports of non-toxicogenic *G. spinifera* in the North Atlantic (Krock et al., 2006) and South Atlantic (Krock et al., 2015). They concluded that the two previous reports of YTX-producing *G. spinifera* are based on misidentifications because the phylogeny locates the toxicogenic strain from New Zealand (Rhodes et al., 2006) closer to *Gonyaulax ellegaardiae* and the toxicogenic strain from South Africa (Pitcher et al., 2019) in the *G. membranaceae* clade. The presence of several different morphotypes of *Spiniferites* in the SMG (corresponding to different species of *Gonyaulax*) raises the question if there are toxicogenic genotypes in the area.

6 Conclusions

In this study, we have provided the first data about the composition and distribution of dinocysts and their link with the environmental parameters of San Matías Gulf, a vulnerable and high priority conservation region. Our results provide a baseline of dinocyst diversity, the factors related to their deposition, and the hydrological conditions that allow the development of recurrent blooms in this relevant area for fisheries. In this gulf, higher abundances of dinocysts, with a dominance of phototrophic species, are found in the inner areas where a gyre system and thermal stratification of the water column develop during spring and summer, creating an environment conducive to cysts and fine sediment deposition. This survey highlights the presence of extensive beds of *P. reticulatum* and *A. catenella* cysts, representing potential risk areas for cysts germination and inoculation of the water column. As the relationship between pelagic and benthic stages is little known, further interdisciplinary studies in the gulf are required involving physical-chemical conditions of the gulf, higher spatial data resolution for dinocyst mapping and plankton analysis. Studies with direct measurements of vertical particle fluxes and bottom circulation are needed to better assess the hydrodynamic processes in the gulf, accompanied by the determination of sedimentation rates.

Data availability statement

The original contributions presented in the study are included in the article/supplementary material. Further inquiries can be directed to the corresponding author.

Author contributions

JX: Conceptualization, Formal Analysis, Investigation, Visualization, Writing – original draft, Writing – review & editing. CB: Conceptualization, Investigation, Methodology, Supervision, Writing – original draft, Writing – review & editing. CF: Data curation, Visualization, Writing – original draft, Writing – review & editing. BK: Conceptualization, Supervision, Writing – original draft, Writing – review & editing.

Funding

The author(s) declare that financial support was received for the research and/or publication of this article. This study was supported

by the Fund for the Scientific and Technological Research (FONCYT-MINCYT), Argentina (PICT 2016-3775 to CB and a Ph.D. fellowship to JX) and the Fund from National Scientific and Technical Research Council (CONICET), Argentina (PIP 0100205). This work is also a contribution to the IGCP-UNESCO Project 681. The publication costs of this article were covered by the Open Access publication fund of Alfred Wegener Institut-Helmholtz Zentrum für Polar- und Meeresforschung.

Acknowledgments

INIDEP for providing historic CTD data, Juan P. Pisoni (CENPAT) and Carlos Balestrini (SHN) for providing calibrated CTD data of CONCACEN and Primavera Patagónica cruises, Gabriela Williams (CENPAT) for offering nitrate data obtained through projects PICT 2003-15221, 2006-1575, 2006-649, and BID-PNUD ARG B-B 60, Pablo Díaz (INGEOSUR) and Julieta Carbonella (IADO) for technical assistance in laboratories, and the R/V Puerto Deseado (CONICET-MINDEF) crew for onboard collaboration. We are also very grateful to the editor, Jin Zhou, as well as Barrie Dale and Zhangxi Hu and two anonymous reviewers, which significantly improved the manuscript with their constructive suggestions.

Conflict of interest

The authors declare that the research was conducted in the absence of any commercial or financial relationships that could be construed as a potential conflict of interest.

Generative AI statement

The author(s) declare that no Generative AI was used in the creation of this manuscript.

Publisher's note

All claims expressed in this article are solely those of the authors and do not necessarily represent those of their affiliated organizations, or those of the publisher, the editors and the reviewers. Any product that may be evaluated in this article, or claim that may be made by its manufacturer, is not guaranteed or endorsed by the publisher.

References

- Acha, E. M., Mianzan, H. W., Guerrero, R. A., Favero, M., and Bava, J. (2004). Marine fronts at the continental shelves of austral South America: physical and ecological processes. *J. Mar. Syst.* 44, 83–105. doi: 10.1016/j.jmarsys.2003.09.005
- Acha, E. M., Piola, A., Iribarne, O., and Mianzán, H. (2015). "Ecological processes at marine fronts: oases in the ocean," in *SpringerBriefs in Environmental Science* (Springer, New York). doi: 10.1007/978-3-319-15479-4

- Akselman, R. (1985). Contribución al estudio de la familia Gymnodiniaceae Lemmermann (Dinophyta) del Atlántico Sudoccidental. *Physis* 43, 39–50.
- Akselman, R. (1986). Contribución al conocimiento de la familia Warnowiaceae Lindenmann (Clase Dinophyceae) del Atlántico sudoccidental. *Darwiniana* 27, 9–17.
- Akselman, R. (1987). Quistes planctónicos de dinofíceas en áreas de plataforma del Atlántico Sudoccidental, I. Reporte taxonómico de la familia Peridiniaceae Ehrenberg. *Bolm. Inst. Oceanog.* 35, 17–32. doi: 10.1590/S0373-55241987000100004
- Akselman, R., Krock, B., Alpermann, T. J., Tilmann, U., Borel, C. M., Almandoz, M. E., et al. (2015). *Protoceratium reticulatum* (Dinophyceae) in the austral Southwestern Atlantic and the first report on YTX-production in shelf waters of Argentina. *Harmful Algae* 45, 40–52. doi: 10.1016/j.hal.2015.03.001
- Amoroso, R., and Gagliardini, D. A. (2010). Inferring complex hydrographic processes using remote-sensed images: turbulent fluxes in the Patagonian gulfs and implication for scallop metapopulation dynamics. *J. Coast. Res.* 2, 243–254. doi: 10.2112/08-1095.1
- Amoroso, R. O., Parma, A. M., Orensanz, J. M., and Gagliardini, D. A. (2011). Zooming the microscope: medium-resolution remote sensing as a framework for the assessment of a small-scale fishery. *ICES J. Mar. Sci.* 68, 696–706. doi: 10.1093/icesjms/fsq162
- Anderson, D. M., Cembella, A. D., and Hallegraeff, G. M. (2012). Progress in understanding harmful algal blooms: Paradigm shifts and new technologies for research, monitoring, and management. *Ann. Rev. Mar. Sci.* 4, 143–176. doi: 10.1146/annurev-marine-120308-081121
- Anderson, D. M., Stock, C. A., Keafar, B. A., Nelson, A. B., Thompson, B., McGillicuddy, D. J. Jr., et al. (2005). *Alexandrium fundyense* cyst dynamics in the Gulf of Maine. *Deep-Sea Res.* 52, 2522–2542. doi: 10.1016/j.dsr.2.2005.06.014
- Antacli, J., Silva, R., Jaureguizar, A., Hernández, D., Mendiolar, M., Sabatini, M., et al. (2018). Phytoplankton and protozooplankton on the southern Patagonian shelf (Argentina, 47°–55°S) in late summer: Potentially toxic species and community assemblage structure linked to environmental features. *J. Sea Res.* 140, 63–80. doi: 10.1016/j.seares.2018.07.012
- Balech, E. (1988). *Los dinoflagelados del Atlántico Sudoccidental* (Madrid: Instituto Español de Oceanografía).
- Brosnahan, M. L., Ralston, D. K., Fischer, A. D., Solow, A. R., and Anderson, D. M. (2017). Bloom termination of the toxic dinoflagellate *Alexandrium catenella*: vertical migration behavior, sediment infiltration, and benthic cyst yield. *Limnol. Oceanogr.* 62, 2829–2849. doi: 10.1002/lno.10664
- Candel, M. S., Radi, T., de Vernal, A., and Bujalesky, G. (2012). Distribution of dinoflagellate cysts and other aquatic palynomorphs in surface sediments from the Beagle Channel, southern Argentina. *Mar. Micropaleontol.* 96–97, 1–12. doi: 10.1016/j.marmicro.2012.06.009
- Carreto, J. I., Benavides, H. R., Negri, R. M., and Glorioso, P. D. (1986). Toxic red tide in the Argentine Sea. Phytoplankton distribution and survival of the toxic dinoflagellate *Gonyaulax excavata* in a frontal area. *J. Plankton Res.* 8, 15–28. doi: 10.1093/plankt/8.1.15
- Carreto, J. I., Lasta, M. L., Negri, R. M., and Benavides, H. R. (1981). “Los fenómenos de Marea Roja y toxicidad de moluscos bivalvos en el Mar Argentino,” in *Campañas de investigación pesquera realizadas en el Mar Argentino por los B/I ‘Shinkai Maru’ y ‘Walter Herwig’ y B/P ‘Marburg’, años 1978 y 1979. Resultados de la Parte Argentina*, vol. 399. Ed. V. Angelescu (Mar del Plata: Ser. Contr. Inst. Nac. Invest. Des. Pesq), 181–201.
- Carreto, J. I., and Verona, C. A. (1974). *Fitoplancton, pigmentos y condiciones ecológicas del Golfo San Matías I. Campaña SAO I (marzo 1971)* Vol. 10 (Mar del Plata: C.I.C. Prov. Bs. As., Contrib. 235, Inst. Biol. Mar. de Mar del Plata. Informe), 1–22.
- Crespi-Abril, A., Morsan, E., and Barón, P. (2008). Contribution to understanding the population structure and maturation of *Illex argentinus* (Castellanos 1960): the case of the inner-shelf spawning groups in San Matías Gulf (Patagonia, Argentina). *J. Shellfish Res.* 27, 1225–1231. doi: 10.2983/0730-8000-27.5.1225
- Dale, B. (1976). Cyst formation, sedimentation, and preservation: Factors affecting dinoflagellate assemblages in recent sediments from Trondheimsfjord, Norway. *Rev. Palaeobot. Palynol.* 22, 39–60. doi: 10.1016/0034-6667(76)90010-5
- Dale, B., Dale, A. L., and Jansen, F. J. H. (2002). Dinoflagellate cysts as environmental indicators in surface sediments from the Congo deep-sea fan and adjacent regions. *Palaeogeog. Palaeoclimatol. Palaeoecol.* 185, 309–338. doi: 10.1016/S0031-0182(02)00380-2
- de Vernal, A. (2009). Marine palynology and its use for studying nearshore environments. *IOP Conf. Series: Earth Environ. Sci.* 5, 012002. doi: 10.1088/1755-1307/5/1/012002
- de Vernal, A., Eynaud, F., Henry, M., Hillaire-Marcel, C., Londeix, L., and Mangin, S., et al. (2005). Reconstruction of sea surface conditions at middle to high latitudes of the Northern Hemisphere during the Last Glacial Maximum (LGM) based on dinoflagellate cyst assemblages. *al. Quat. Sci. Rev.* 24, 897–924. doi: 10.1016/j.quascirev.2004.06.014
- de Vernal, A., Henry, M., and Bilodeau, G. (2010). “Micropaleontological preparation techniques and analyses,” in *Les Cahiers du GEOTOP, 3rd ed.*, vol. 3. (Département des Sciences de la Terre, UQAM, Montreal).
- de Vernal, A., and Marret, F. (2007). “Organic-walled dinoflagellate cysts: tracers of sea-surface conditions,” in *Developments in Marine Geology*. Eds. C. Hillaire-Marcel and A. Vernal (Elsevier, Amsterdam), 371–408.
- de Vernal, A., Rochon, A., and Radi, T. (2007). “Dinoflagellates,” in *Encyclopedia of Quaternary Science*. Ed. S. A. Elias (Elsevier, Amsterdam), 1652–1667. doi: 10.1016/B044-452747-8/00300-8
- Ellegaard, M., Daugbjerg, N., Rochon, A., Lewis, J., and Harding, A. I. (2003). Morphological and LSU rDNA sequence variation within the *Gonyaulax spiniferes* group (Dinophyceae) and proposal of *G. elongata* comb. nov. and *G. membranacea* comb. nov. *Phycologia* 42, 151–164. doi: 10.2216/i0031-8884-42-2-151.1
- Ellegaard, M., and Ribeiro, S. (2018). The long-term persistence of phytoplankton resting stages in aquatic ‘seed banks’. *Biol. Rev.* 93, 166–183. doi: 10.1111/brv.12338
- Esteves, J., Santinelli, N., Sastre, V., Diaz, R., and Rivas, O. (1992). A toxic dinoflagellate bloom and PSP production associated with upwelling in Golfo Nuevo, Patagonia Argentina. *Hydrobiologia* 242, 115–122. doi: 10.1007/BF00018067
- Fabro, E., and Almandoz, G. (2021). Field observations on rare or overlooked dinoflagellates from the Argentine Sea. *Bol. Soc Argent. Bot.* 56, 123–140. doi: 10.31055/1851.2372.v53.n4.21978
- Fabro, E., Almandoz, G., Ferrario, M., John, U., Tillmann, U., Toebe, K., et al. (2017). Morphological, molecular, and toxin analysis of field populations of *Alexandrium* genus from the Argentine Sea. *J. Phycol.* 53, 1206–1222. doi: 10.1111/jpy.12574
- Fabro, E., Krock, B., and Almandoz, G. (2018). Dinoflagelados productores de yessotoxinas en el Mar Argentino. *Bol. Soc Argent. Bot.* 53, 551–566. doi: 10.31055/1851.2372.v53.n4.21978
- Faye, S., Rochon, A., and St-Onge, G. (2018). Distribution of modern dinoflagellate cyst assemblages in surface sediments of San Jorge Gulf (Patagonia, Argentina). *Oceanography* 31, 122–131. doi: 10.5670/oceanog.2018.416
- Feifel, K. M., Fletcher, S. J., Watson, L. R., Moore, S. K., and Lessard, E. J. (2015). *Alexandrium* and *Scrippsiella* cyst viability and cytoplasmic fullness in a 60-cm sediment core from Sequim Bay, WA. *Harmful Algae* 47, 56–65. doi: 10.1016/j.hal.2015.05.009
- Fensome, R. A., Taylor, F. J. R., Norris, G., Sarjeant, W. A. S., Wharton, D. I., and Williams, G. L. (1993). *A classification of fossil and living dinoflagellates* (New York: Micropaleontology Press Special Paper).
- Figuerola, R. I., Rengefors, K., and Bravo, I. (2006). Effects of parental factors and meiosis on sexual offspring of *Gymnodinium nollerii* (Dinophyceae). *J. Phycol.* 42, 350–362. doi: 10.1111/j.1529-8817.2006.00191.x
- Gagliardini, D., and Rivas, A. (2004). Environmental characteristic of San Matías Gulf obtained from LANDSAT-TM and ETM+ data. *Gayana* 68, 186–193. doi: 10.4067/S0717-65382004000200034
- Garreaud, R. D. (2009). The andes climate and weather. *Adv. Geosci.* 7, 1–9. doi: 10.5194/adgeo-22-3-2009
- Garreaud, R. D., Vuille, M., Campagnucci, R., and Marengo, J. (2009). Present-day South American climate. *Palaeogeog. Palaeoclimatol. Palaeoecol.* 281, 180–195. doi: 10.1016/j.palaeo.2007.10.032
- Gayoso, A. M., and Fulko, V. K. (2006). Observations on *Alexandrium tamarense* (Lebour) Balech and other dinoflagellate populations in Golfo Nuevo, Patagonia (Argentina). *J. Plankton Res.* 23, 463–468. doi: 10.1016/j.hal.2004.12.010
- Glibert, P. M., and Mitra, A. (2022). From webs, loops, shunts, and pumps to microbial multitasking: evolving concepts of marine microbial ecology, the mixoplankton paradigm, and implications for a future ocean. *Limnol. Oceanogr.* 67, 585–597. doi: 10.1002/lno.12018
- Grimm, E. C. (1990). “Tilia and tiliagraph,” in *PC spreadsheet and graphic software for pollen data*, vol. 4. (Illinois State Museum IL, USA: INQUA Working Group on Data Handling Methods, Newsletter), 5–7.
- Gu, H., Huo, K., Krock, B., Bilien, G., Pospelova, V., Li, Z., et al. (2021). Cyst-theca relationships of *Spiniferites bentorii*, *S. hyperacanthus*, *S. ramosus*, *S. scabratus* and molecular phylogenetics of *Spiniferites* and *Tectatodinium* (Gonyaulacales, Dinophyceae). *Phycologia* 60, 332–353. doi: 10.1080/00318884.2021.1930796
- Hammer, Ø., Harper, D. A. T., and Ryan, P. D. (2001). PAST: paleontological statistics software package for education and data analysis. *Palaeontol. Electron.* 4, 9. Available online at: http://palaeo-electronica.org/2001_1/past/issue1_01.htm.
- Hansen, P. J. (2011). The role of photosynthesis and food uptake for the growth of marine mixotrophic dinoflagellates. *J. Eukaryot. Microbiol.* 58, 203–214. doi: 10.1111/j.1550-7408.2011.00537.x
- Hernández-Moresino, R. D., Crespi-Abril, A. C., Soria, G., Sánchez, A., Isla, F., and Barón, P. J. (2019). Inferring bottom circulation based on sediment pattern distribution in the San José Gulf, Patagonia Argentina. *J. South Am. Earth Sci.* 89, 189–196. doi: 10.1016/j.jsames.2018.10.013
- Hoffmeyer, M. S., Dutto, M. S., Berasategui, A. A., García, M. D., Pettigrosso, R. E., Almandoz, G. O., et al. (2020). DOMOIC acid, *Pseudo-nitzschia* spp and potential vectors at the base of the pelagic food web over the northern Patagonian coast, Southwestern Atlantic. *J. Mar. Syst.* 212, 103448. doi: 10.1016/j.jmarsys.2020.103448
- Howe, J. A., Harland, R., Cottier, F. R., Brand, T., Willis, K. J., Berge, J. R., et al. (2010). Dinoflagellate cysts as proxies for palaeoceanographic conditions in Arctic fjords. *Geol. Soc Spec. Publ.* 344, 61–74. doi: 10.1144/SP344.6
- INDEC - Instituto Nacional de Estadística y Censos (2010). *Censo Nacional de población, Hogares y Viviendas*, Vol. 2010.
- Jephson, T., Fagerberg, T., and Carlsson, P. (2011). Dependency of dinoflagellate vertical migration on salinity stratification. *Aquat. Microb. Ecol.* 63, 255–264. doi: 10.3354/ame01498

- Kelley, D. A., Richards, C., and Layton, C. (2022). oce: an R package for oceanographic analysis. *J. Open Res. Software* 7, 3594. doi: 10.21105/joss.03594
- Kremp, A., and Anderson, D. M. (2000). Factors regulating germination of resting cysts of the spring bloom dinoflagellate *Scrippsiella hangoei* from the northern Baltic Sea. *J. Plankton Res.* 22, 1311–1327. doi: 10.1093/plankt/22.7.1311
- Krock, B., Alpermann, T. J., Tillmann, U., Pitcher, G. C., and Cembella, A. D. (2006). “Yessotoxin profiles of the marine dinoflagellates *Protoceratium reticulatum* and *Gonyaulax spinifera*,” in *12th International Conference on Harmful Algae* (ISSHA and IOC of UNESCO, Copenhagen, Denmark).
- Krock, B., Borel, C. M., Barrera, F., Tillmann, U., Fabro, E., Almandoz, G., et al. (2015). Analysis of the hydrographic conditions and cyst beds in the San Jorge Gulf, Argentina, that favour dinoflagellate population development including toxicogenic species and their toxins. *J. Mar. Syst.* 148, 86–100. doi: 10.1016/j.jmarsys.2015.01.006
- Labraga, J. C., and Villalba, R. (2009). Climate in the Monte Desert: Past trends, present conditions, and future projections. *J. Arid Environ.* 73, 154–163. doi: 10.1016/j.jaridenv.2008.03.016
- Marmorino, G., Chen, W., and Mied, R. P. (2017). Submesoscale tidal-inlet dipoles resolved using stereo worldview imagery. *IEEE Geosci. Remote Sens. Lett.* 14, 1705–1709. doi: 10.1109/LGRS.2017.2729886
- Marret, F., Bradley, L., de Vernal, A., Hardy, W., Kim, S., Mudie, P., et al. (2019). From bipolar to regional distribution of modern dinoflagellate cysts, an overview of their biogeography. *Mar. Micropaleontol.* 159, 101753. doi: 10.1016/j.marmicro.2019.101753
- Marret, F., and Zonneveld, K. A. F. (2003). Atlas of modern organic-walled dinoflagellate cyst distribution. *Rev. Palaeobot. Palynology* 125, 1–20. doi: 10.1016/S0034-6667(02)00229-4
- Martinetto, P., Daleo, P., Escapa, M., Alberti, J., Isacch, J. P., Fanjul, E., et al. (2010). High abundance of consumers associated with eutrophic areas in a semi-desert macrotidal coastal ecosystem in Patagonia, Argentina. *Estuar. Coast. Shelf Sci.* 88, 357–364. doi: 10.1016/j.ecss.2010.04.012
- Matsuoka, K., and Fukuyo, Y. (2000). *Technical guide for modern dinoflagellate cyst study* (Tokyo: WESTPAC-HAB/WESTPAC/IOC, Asian Natural Environmental Science Center).
- Matthiessen, J., De Vernal, A., Head, M., Okolodkov, Y., Zonneveld, K., and Harland, R. (2005). Modern organic-walled dinoflagellate cysts in Arctic marine environments and their (paleo-) environmental significance. *Palaentolog. Z.* 79, 3–51. doi: 10.1007/BF03021752
- Miyazono, A., Nagai, S., Kudo, I., and Tanizawa, K. (2012). Viability of *Alexandrium tamarense* cysts in the sediment of Funka Bay, Hokkaido, Japan: over a hundred-year survival times for cysts. *Harmful Algae* 16, 81–88. doi: 10.1016/j.hal.2012.02.001
- Mouzo, F., and Paterlini, C. (2017). Geología submarina del Golfo Norpatagónico San Matías. *Rev. Asoc. Geol. Arg.* 74, 553–569. Available online at: <https://revista.geologica.org.ar/raga/article/view/193>.
- Ocampo-Reinaldo, M., González, R., Williams, G., Storero, L. P., Romero, M. A., Narvarte, M., et al. (2013). Spatial patterns of the Argentine hake *Merluccius hubbsi* and oceanographic processes in a semi-enclosed Patagonian ecosystem. *Mar. Biol. Res.* 9, 394–406. doi: 10.1080/17451000.2012.739700
- Orozco, F. E., and Carreto, J. I. (1989). “Distribution of *Alexandrium excavatum* cyst in a Patagonic area (Argentina),” in *Red Tides: Biology, Environmental Science and Toxicology*. Eds. T. Okaichi, D. M. Anderson and T. Nemoro (Elsevier Science Publishing, New York), 309–312.
- Piola, A. R., and Rivas, A. L. (1997). “Corrientes en la plataforma continental,” in *El Mar Argentino y sus recursos pesqueros*, vol. 1. Ed. E. E. Boschi (INIDEP, Mar del Plata), 119–132.
- Piola, A., and Scasso, L. (1988). Circulación en el Golfo San Matías. *Geoacta* 16, 35–51.
- Pisoni, J., Rivas, A., and Piola, A. (2015). On the variability of tidal fronts on a macrotidal continental shelf, Northern Patagonia, Argentina. *Deep Sea Res. Part II* 119, 61–68. doi: 10.1016/j.dsr2.2014.01.019
- Pitcher, G. C., Foord, C. J., Macey, B. M., Mansfield, L., Mouton, A., Smith, M. E., et al. (2019). Devastating farmed abalone mortalities attributed to yessotoxin-producing dinoflagellates. *Harmful Algae* 81, 30–41. doi: 10.1016/j.hal.2018.11.006
- Pospelova, V., and Kim, S. (2010). Dinoflagellate cysts in recent estuarine sediments from aquaculture sites of southern South Korea. *Mar. Micropaleontol.* 76, 37–51. doi: 10.1016/j.marmicro.2010.04.003
- R Development Core Team (2021). *R: A language and environment for statistical computing* (Vienna, Austria: R Foundation for Statistical Computing). Available at: <https://www.R-project.org/>.
- Radi, T., and de Vernal, A. (2004). Dinocyst distribution in surface sediments from the northeastern Pacific margin (40–60°N) in relation to hydrographic conditions, productivity and upwelling. *Rev. Palaeobot. Palynol.* 28, 169–193. doi: 10.1016/S0034-6667(03)00118-0
- Rhodes, L., McNabb, P., de Salas, M., Briggs, L., Beuzenberg, V., and Gladstone, M. (2006). Yessotoxin production by *Gonyaulax spinifera*. *Harmful Algae* 5, 148–155. doi: 10.1016/j.hal.2005.06.008
- Richerol, T., Pienitz, R., and Rochon, A. (2012). Modern dinoflagellate cyst assemblages in surface sediments of Nunatsiavut fjords (Labrador, Canada). *Mar. Micropaleontol.* 88, 54–64. doi: 10.1016/j.marmicro.2012.03.002
- Romero, M. A., Ocampo-Reinaldo, M., Williams, G., Narvarte, M., Gagliardini, D. A., and González, R. (2013). Understanding the dynamics of an enclosed trawl demersal fishery in Patagonia (Argentina): A holistic approach combining multiple data sources. *Fish Res.* 140, 73–82. doi: 10.1016/j.fishres.2012.12.002
- Saraceno, M., Tonini, M. H., Williams, G. N., Aubone, N., Olascoaga, M. J., Beron-Vera, F. J., et al. (2020). On the complementary information provided by satellite images, lagrangian drifters, and a regional numerical model: A case study in the san matias gulf, Argentina. *Remote Sens. Earth Syst. Sci.* 3, 123–135. doi: 10.1007/s41976-020-00039-6
- Sastre, A. V., Santinelli, N. H., Solis, M. E., Pérez, L. B., Díaz Ovejero, S. D., Villalobos, L. G., et al. (2018). “Harmful marine microalgae in coastal waters of Chubut (Patagonia, Argentina),” in *Plankton Ecology of the Southwestern Atlantic: From the Subtropical to the Subantarctic Realm*. Ed. M. S. Hoffmeyer (Springer International Publishing AG, Cham), 495–515. doi: 10.1007/978-3-319-77869-3
- Schlitzer, R. (2021). *Ocean Data View*. Available online at: <https://odv.awi.de> (Accessed May 19, 2023).
- Shepard, F. P. (1954). Nomenclature based on sand-silt-clay ratios. *J. Sediment* 24, 151–158.
- Smayda, T. J. (1997). Harmful algal blooms: Their ecophysiology and general relevance to phytoplankton blooms in the sea. *Limnol. Oceanogr.* 42, 1137–1153. doi: 10.4319/lo.1997.42.5_part_2.1137
- Smayda, T. J. (2002). Turbulence, watermass stratification and harmful algal blooms: an alternative view and frontal zones as “pelagic seed banks. *Harmful Algae* 1, 95–112. doi: 10.1016/S1568-9883(02)00010-0
- Stockmarr, J. (1971). Tablets with spores used in absolute pollen analysis. *Pollen Spores* 13, 615–621.
- Svendsen, G., Romero, A., Williams, G. N., Gagliardini, D. A., Crespo, E., Dans, S., et al. (2015). Environmental niche overlap between common and dusky dolphins in North Patagonia, Argentina. *PLoS One* 10 (6), e0126182. doi: 10.1371/journal.pone.0126182
- Tang, Y. Z., and Gobler, C. J. (2012). The toxic dinoflagellate *Cochlodinium polykrikoides* (Dinophyceae) produces resting cysts. *Harmful Algae* 20, 71–80. doi: 10.1016/j.hal.2012.08.001
- Tonini, M., Palma, E., and Piola, A. (2013). A numerical study of gyres, thermal fronts and seasonal circulation in austral semi-enclosed gulfs. *Cont Shelf Res.* 65, 97–110. doi: 10.1016/j.csr.2013.06.011
- Wentworth, C. K. (1922). A scale of grade and class terms for clastic sediments. *J. Geol.* 30, 377–392. doi: 10.1086/622910
- Williams, G., Pisoni, J., Solis, M., Romero, M., Ocampo-Reinaldo, M., Svendsen, G., et al. (2021). Variability of phytoplankton biomass and environmental drivers in a semi-enclosed coastal ecosystem (San Matías Gulf, Patagonian Continental Shelf, Argentina) using ocean color remote sensing (MODIS) and oceanographic field data: Implications for fishery resources. *J. Mar. Sys.* 224, 103615. doi: 10.1016/j.jmarsys.2021.103615
- Williams, G., Sapoznik, M., Ocampo-Reinaldo, M., Solis, M., Narvarte, M., González, R., et al. (2010). Comparison of AVHRR and SeaWiFS imagery with fishing activity and in situ data in San Matías Gulf, Argentina. *Int. J. Remote Sens* 31, 4531–4542. doi: 10.1080/01431161.2010.485218
- Zonneveld, K., Hoek, R., Brinkhuis, H., and Willems, H. (2001). Geographical distribution of organic-walled dinoflagellate cysts in surficial sediments of the Benguela upwelling region and their relationship to upper ocean conditions. *Prog. Oceanogr.* 48, 25–72. doi: 10.1016/S0079-6611(00)00047-1
- Zonneveld, K., Marret, F., Versteegh, G., Bogus, K., Bonnet, S., Bouimetarhan, I., et al. (2013). Atlas of modern dinoflagellate cyst distribution based on 2405 data points. *Rev. Palaeobot. Palynol.* 191, 1–197. doi: 10.1016/j.revpalbo.2012.08.003
- Zonneveld, K., and Pospelova, V. (2015). A determination key for modern dinoflagellate cysts. *Palynology* 39, 387–409. doi: 10.1080/01916122.2014.990115